Data report: whole-rock major and trace elements and mineral compositions of the sheeted dike–gabbro transition in ODP Hole 1256D[1]

Shusaku Yamazaki,[2] Natsuki Neo,[2] and Sumio Miyashita[2]

Chapter contents

[1]Yamazaki, S., Neo, N., and Miyashita, S., 2009. Data report: whole-rock major and trace elements and mineral compositions of the sheeted dike–gabbro transition in ODP Hole 1256D. *In* Teagle, D.A.H., Alt, J.C., Umino, S., Miyashita, S., Banerjee, N.R., Wilson, D.S., and the Expedition 309/312 Scientists, *Proc. IODP,* 309/312: Washington, DC (Integrated Ocean Drilling Program Management International, Inc.). doi:10.2204/iodp.proc.309312.203.2009
[2]Graduate School of Science and Technology, Niigata University, 8050 Ikarashi 2, Niigata 950-2181, Japan. Correspondence author: **shu-saku@mvd.biglobe.ne.jp**

Abstract

We analyzed whole-rock major element, trace element, and mineral compositions of basalt and gabbro samples recovered from Ocean Drilling Program (ODP) Hole 1256D during Integrated Ocean Drilling Program Expedition 312. Hole 1256D, located at ODP Site 1256 in the eastern equatorial Pacific, is drilled into ~15 Ma oceanic crust at the East Pacific Rise, which was formed during a period of superfast spreading (up to 220 mm/y full rate). The analyzed samples were collected from the upper dikes (1255–1348.3 meters below seafloor [mbsf]), granoblastic dikes (1348.3–1406.6 mbsf), Gabbro 1 (1406.6–1458.9 mbsf), the upper dike screen (1458.9–1483.1 mbsf), Gabbro 2 (1483.1–1495 mbsf), and the lower dike screen of uncertain origin (1495–1507.1 mbsf). Whole-rock compositions were measured for 19 basalts and 13 gabbros by X-ray fluorescence and inductively coupled plasma–mass spectrometry. Mineral compositions were analyzed for 18 basalts and 24 gabbros by electron probe X-ray microanalysis. Results show the geochemical characteristics of each lithology and the downhole variations from the sheeted dike complex to gabbros in a superfast spreading oceanic crust. The upper dikes, granoblastic dikes, and upper dike screen have similar normal mid-ocean-ridge basalt (N-MORB)-like trace element patterns. However, the plagioclase MgO contents of the granoblastic dikes and upper dike screen are notably lower than those of the sheeted dikes. The lower dike screen has a unique P-, Zr-, Hf-, and light rare earth element–depleted character. On the other hand, clinopyroxene and plagioclase compositions resemble those of the granoblastic dikes and the upper dike screen. Gabbros 1 and 2 have almost the same N-MORB–normalized trace element patterns, though their La/Sm ratios differ. Clinopyroxene TiO_2 and the zoning of olivine Fo content also differ between Gabbros 1 and 2. Downhole variations show that Gabbro 1 decreases in whole-rock TiO_2, P_2O_5, and Zr content and increases in pyroxene Mg# ($100 \times Mg/[Mg + Fe]$), except for the most differentiated sample in the middle part of Gabbro 1.

Introduction

This report provides the results of geochemical analyses of basalt and gabbro shipboard samples recovered during Integrated Ocean Drilling Program (IODP) Expedition 312 from Ocean Drilling Pro-

doi:10.2204/iodp.proc.309312.203.2009

gram (ODP) Hole 1256D. Hole 1256D is in the oceanic crust of the Cocos plate, which was formed by superfast spreading at the East Pacific Rise (220 mm/y full spreading rate) at 15 Ma. Hole 1256D was deepened to 1507.1 meters below seafloor (mbsf) during three combined expeditions: ODP Leg 206 and IODP Expeditions 309 and 312. These expeditions succeeded in collecting gabbro samples from an upper oceanic crust sequence composed of deep-sea sediment, pillow and lava flows, and sheeted dikes.

During Expedition 312, drilling was started in the sheeted dikes at 1255 mbsf. The lowermost 60 m was partially or completely recrystallized. Because these sheeted dikes are characterized by distinctive granoblastic textures with secondary mineral assemblages of plagioclase, clinopyroxene, orthopyroxene, amphibole, and Fe-Ti oxide, they were classified as the "granoblastic dikes" (Wilson et al., 2006). At 1406.6 mbsf, drilling in Hole 1256D encountered a felsic plutonic rock intruded into the granoblastic dikes. This depth is regarded as the beginning of the "plutonic complex" (Wilson et al., 2006). The plutonic complex includes two gabbroic intervals (52.3 m thick upper Gabbro 1 and 24 m thick lower Gabbro 2) separated by the 24.2 m thick upper dike screen (see **"Igneous petrology"** in the "Site 1256" chapter). The lower portion of Gabbro 2 consists of a 12.1 m thick gabbronorite of uncertain origin. We hereafter refer to this gabbronorite unit as the lower dike screen, which is assigned to metamorphosed basalt dike screen in the **"Site 1256"** chapter.

A data set of geochemical analysis of the sheeted dikes–gabbro transition in Hole 1256D gives basic information for understanding the magmatic, metamorphic, and hydrothermal systems beneath the superfast spreading ridge.

Methods and materials

Sample description

This report presents the whole-rock major and trace element compositions of 32 samples (19 basalts and 13 gabbros) and mineral compositions of 42 samples (18 basalts and 24 gabbros) obtained during Expedition 312. On the basis of microscopic observations, we selected samples with the minimum amount of secondary minerals such as chlorite, epidote, and albite so that primary igneous mineral compositions are well preserved for electron probe microanalysis. Analyzed samples are listed in Table **T1.**

The lithologic features of the samples are as follows. The dikes, which were recovered from Hole 1256D during Expedition 312, are metamorphosed to various grades from greenschist to pyroxene hornfels facies (see **"Igneous petrology"** in the "Site 1256" chapter). The development of the secondary minerals of Hole 1256D basalts and dolerites is classified into eight types in the **"Site 1256"** chapter and by Koepke et al. (2008). This report follows this classification, based on the primary igneous features of glass, clinopyroxene, plagioclase, and Fe-Ti oxides and secondary mineral assemblages of dusty brown material (mostly actinolite), amphibole, clinopyroxene, orthopyroxene, and Fe-Ti oxides. Type 1 is defined as completely fresh basalt with pristine glass and phenocrysts. Type 2 is characterized by the appearance of secondary minerals after glass. Type 3 is defined as slightly altered basalt where glass is altered to chlorite and oxides and <50% of primary clinopyroxene is altered to the dusty brown fibrous masses, while plagioclase is mostly primary. Type 4 is defined as the much-altered basalt in which >50% clinopyroxene is altered to dusty brown fibrous masses and Fe-Ti oxides and plagioclase is altered to dusty brown material. Type 5 is characterized by the first appearance of granular clinopyroxene, orthopyroxene, and green flaky hornblende as secondary minerals. This type is defined as metamorphosed basalt in which >90% clinopyroxene is altered to actinolite and oxide and plagioclase is replaced by submicrometer-size discrete Fe-Ti oxides and actinolite. Type 6 is defined as metamorphosed basalt where primary clinopyroxene is completely altered to prismatic actinolite, green to brown flaky hornblende, and Fe-Ti oxides grains. Types 7 and 8 are mature metabasalt. Type 7 is defined by microgranular mosaic-like texture with typical granoblastic domains, flaky and poikiloblastic green to brown hornblende, and prismatic actinolite. The typical granoblastic domain consists of microgranular clinopyroxene, orthopyroxene, and Fe-Ti oxides. Type 8 metabasalt is characterized by more or less continuous microgranular granoblastic mosaics of secondary clinopyroxene, orthopyroxene, plagioclase, hornblende, and Fe-Ti oxides (for details, see table 3 of Koepke et al., 2008). These types correspond to metamorphic grade from greenschist facies (Type 3) up to pyroxene hornfels facies (Type 7 and 8). The analyzed samples include Type 3, 4, 6, 7, and 8. The majority of the sheeted dikes are Type 3 and 4 basalts, except that the granoblastic dikes are Type 7. The upper dike screen consists of Type 8 metabasalt. Under a microscope, it is not clear whether three samples (312-1256D-233R-1, 4–7 cm, and 234R-1, 1–2 and 7–9 cm) from the lower dike screen are of igneous or metamorphic origin (see **"Igneous petrology"** in the "Site 1256" chapter). These rocks show a microgranular texture with granular clinopyroxene, orthopyroxene, plagioclase, and Fe-Ti oxide and include 0.5 to 1.5 mm long phenocryst-like prismatic plagioclase

relics that include submicrometer-scale spherical Fe-Ti oxides and transparent inclusions (Fig. F1G, F1H). Because this mineral assemblage, texture, and appearance of phenocryst relics resemble the characteristics of the Type 8 metabasalts of the upper dike screen, these samples are classified as Type 8 metabasalt.

Gabbro 1 mainly consists of disseminated oxide orthopyroxene-bearing olivine gabbro. Gabbro 1 gabbros commonly carry Fe-Ti oxide, which decreases with depth. Olivine is present in significant amounts in the lower portions of Gabbro 1, whereas orthopyroxene is not abundant and is largely associated with olivine. Some of the large orthopyroxenes include numerous bleb-like clinopyroxene intergrowths a few micrometers in size. The clinopyroxenes of Gabbro 1 are anhedral or poikilitic between subhedral plagioclase frameworks. Multiple zoning is observed in large subhedral plagioclases. Gabbro 1 clinopyroxenes are largely altered to green or greenish brown amphibole with Fe-Ti oxide. The upper part of Gabbro 1 (Units 83 and 85) has the development of a patchy texture with clinopyroxene-rich subophitic domain and plagioclase-rich coarse-grained patch or network domain (Fig. F32 in the "Site 1256" chapter). The subophitic domain is characterized by clinopyroxene oikocrysts roughly 5 to 10 mm across with up to a few millimeter long plagioclase chadocrysts. The coarse-grained domain is characterized by coarser grained zoned euhedral prismatic plagioclase and abundant Fe-Ti oxide (Fig. F2). The subophitic domain rarely contains orthopyroxene. Remarkable exsolution lamellae occur in some of the clinopyroxenes in the coarse-grained domain. The clinopyroxene with the lamellae occurs in the rim of the subophitic clinopyroxene at the contact between the two domains (Fig. F1A, F1B). The alteration minerals in Gabbro 1 are dominated by albite, chlorite, epidote, calcite, green amphibole, and Fe-Ti oxides.

Gabbro 2 mainly consists of orthopyroxene-bearing gabbro, characterized by variable orthopyroxene content up to 20%. Fe-Ti oxides are present up to 5% and generally decrease with depth. Plagioclase is euhedral to subhedral with a simply or oscillatory zoned clouded core that includes numerous submicrometer opaque inclusions (Fig. F1C). In the metabasalts and Gabbros 1 and 2, clinopyroxene is classified into three types: igneous-type, amphibole-intergrowth (amphibole-type), and pale green colored (secondary-type). Igneous-type clinopyroxene is characterized by the existence of exsolution lamellae partly filled with opaque minerals (Fig. F1E). Amphibole-type clinopyroxene is variably replaced by greenish brown to brown amphiboles and Fe-Ti oxides a few to a few tens of micrometers in diameter (Fig. F1D). Secondary-type clinopyroxene is more transparent than the other types. This type is rarely observed in Type 7 metabasalt in Gabbro 1 and the upper and lower dike screen and rarely occurs as a cluster or vein (Fig. F1F). These secondary-type clinopyroxenes are observed as the pale green colored poikiloblasts which form veins or clusters and are sharply distinguished from the other types by their extremely low TiO_2 content (see "Clinopyroxene"). This pale green clinopyroxene with extremely low TiO_2 has been reported as secondary mineral in the granoblastic dikes because of retrograde metamorphism (Koepke et al., 2008). Gabbro 2 orthopyroxenes are anhedral and enclose or partially enclose euhedral plagioclases. Some large orthopyroxenes include clinopyroxene bleb-like intergrowths. Olivine rarely presents in Gabbro 2 and most olivine is pseudomorphed with iddingsite and iron oxide or talc, green to brown amphibole, and opaque minerals. Olivine commonly occurs with orthopyroxene and opaque minerals. Some olivines are poikilitically enclosed by large anhedral orthopyroxenes. Gabbro 2 includes some metabasalt or rounded metabasalt enclaves up to 1 cm in diameter (e.g., Sample 312-1256D-230R-1, 81–84 cm; 1483.81 mbsf). The texture of the enclaves corresponds to Type 7 or 8 metabasalt, which is similar to the lower dike screen. Gabbro 2 alteration minerals are dominated by greenish brown to brown amphibole and Fe-Ti oxide.

Methods

Sample preparation

Samples were prepared for X-ray fluorescence (XRF) and inductively coupled plasma–mass spectrometry (ICP-MS) as follows. To minimize the effect of alteration, visibly weathered parts and hydration veins were removed. Processed chips were washed for 15 min in an ultrasonic bath filled with ion-exchanged water and then dried for >24 h in an oven at 120°C. Dried samples were crushed using a tungsten carbide mortar followed by milling in a tungsten carbide ball mill. W, Co, Ta, and Nb were excluded from trace element analysis because of possible contamination from the tungsten carbide.

Major elements

Major elements (SiO_2, Al_2O_3, TiO_2, FeO [total Fe as FeO], MnO, CaO, MgO, Na_2O, K_2O, and P_2O_5) were analyzed with a Rigaku RIX-3000 X-ray fluorescence spectrometer at the Faculty of Science, Niigata University (Japan). Powdered samples were dried at 120°C for 1 h to remove H_2O and heated for a further 12 h at 900°C in a muffle furnace to obtain loss-on-ignition (LOI) values. A heated powder sample (0.5 g) was mixed with 5 g $Li_2B_4O_7$ and fused in a platinum crucible at 1200°C to form a glass bead.

Calibration curves were made using the Geological Survey of Japan (GSJ) igneous rock series standard samples. To include a wide range of compositions, some standard samples were synthesized by adding pure chemical agents to GSJ standard samples (for example, pure TiO_2 was added to the JB-1b standard). The precision of analysis was verified by multiple measurements of the JB-2 standard (Table T2). These measured values are in good agreement with the reference values (Imai et al., 1995; Eggins et al., 1997).

Trace elements

Trace elements were analyzed using the ICP-MS Agilent 7500a at the Graduate school of Science and Technology, Niigata University. The elements measured were Sc, V, Ga, Rb, Sr, Y, Zr, Cs, Ba, La, Ce, Pr, Nd, Sm, Eu, Gd, Tb, Dy, Ho, Er, Yb, Lu, Hf, Th, and U. An alkali fusion method was used, following Roser et al. (2000), to avoid residue of acid-resistant minerals such as zircon. However, nitric acid was used instead of the perchloric acid used in the original method. The US Geological Survey (USGS) reference material BHVO-2 was used as a standard for the correction. The precision of the analysis was verified by multiple measurements of the USGS reference material W-2. Results are shown in Table T2.

Mineral composition

Main mineral phases were analyzed by the JXA-8600SX EPMA at the Graduate School of Science and Technology, Niigata University. Plagioclase, clinopyroxene, and orthopyroxene were analyzed for SiO_2, TiO_2, Al_2O_3, Cr_2O_3, FeO, MnO, MgO, CaO, Na_2O, K_2O, BaO, and NiO under the following analytical conditions: acceleration voltage = 15 kV, probe current = 13 nA, and beam diameter = 1 µm. Olivine was analyzed for SiO_2, TiO_2, Al_2O_3, Cr_2O_3, FeO, MnO, MgO, CaO, and NiO under 25 kV and 20 nA with a beam diameter of ~3 µm. Both natural and synthetic oxides and silicates were used as standards. Correction was made according to the ZAF (Z = atomic number, A = absorption, and F = fluorescence) method. Core and rim compositions were obtained from each mineral phase. Analyses of small grains and anhedral minerals were done irrespective of the core and rim. Detection limits are listed in Table T3.

Results

Major elements

Type 3 to 8 basalts and metabasalts show similar variations in the major elements, such as Mg# versus SiO_2, TiO_2, and P_2O_5 (Fig. F3). Higher grade Type 7 and 8 metabasalts have slightly lower K_2O and Mg# than lower grade Type 3 and 4 basalts. Type 3 and 4 samples (312-1256D-176R-1, 21–24 cm, at 1276.29 mbsf and 186R-1, 33–36 cm, at 1319.82 mbsf) have slightly higher LOI values (2.36 and 1.18 wt%, respectively) and notably high K_2O content (0.16 and 0.19 wt%, respectively) (Fig. F3B). This indicates that some elements such as K_2O and Na_2O had been affected by alteration. It is noted that K_2O and LOI are well correlated for those with LOI <0.8 wt%, whereas K_2O is scattered at higher LOIs. The plots characterized by very low LOI and K_2O are exclusively highly recrystallized dikes such as Type 7 and 8 metabasalts. The high-LOI (>0.8 wt%) samples had no clear correlation between K_2O, Na_2O, and LOI. Irrespective to rock types, a strong negative correlation is apparent between Mg# and TiO_2 (Fig. F3C). Gabbro 1 shows wider spectra of SiO_2 and Mg# (SiO_2 = 48.4–51.4 wt%, Mg# = 56–72) than Gabbro 2 (SiO_2 = 49.9–51 wt%, Mg# = 61–63). The highest SiO_2 value (51.4 wt%) occurs at 1440.21 mbsf in the lower middle of the Gabbro 1 subunit. This sample is a slightly altered orthopyroxene-bearing gabbro (Sample 312-1256D-221R-1, 61–64 cm; 1440.21 mbsf) with notably high P_2O_5 (0.17 wt%) and TiO_2 (1.56 wt%) contents. Type 8 metabasalts from the lower dike screen in the lowermost part of Hole 1256D show very low P_2O_5 contents that plot away from the main trend of Mg# versus P_2O_5 variation (Fig. F3D), although they plot on the main trend in the TiO_2-Mg# diagram. Downhole variations of major and trace elements are plotted in Figure F4. The SiO_2, Mg#, TiO_2, and P_2O_5 contents of the dike screen Type 8 metabasalts plot within the range of other metabasalts. Gabbro 1 shows a decreasing trend of TiO_2 and P_2O_5 downhole, except for the sample with the highest P_2O_5 content.

Trace elements

Both Zr and Zr/Y show similar downhole variations to those of P_2O_5 (Fig. F4E, F4F). Type 3 to 7 metabasalts show N-MORB-like patterns for rare earth elements (REE), Sr, P, Zr, Hf, and Y (Fig. F5). Concentrations of these elements are higher in Type 6 and 7 basalts than in Type 3 and 4 basalts (Fig. F5A). U, Th, and Ba values of Type 3 to 7 basalts and metabasalts are slightly higher than the N-MORB values (N-MORB–normalized U = 0.8–2.08, Th = 1.09–2.54, and Ba = 0.99–5.67). The two low-grade metabasalts (Samples 312-1256D-176R-1, 21–24 cm, at 1276.29 mbsf and 186R-1, 33–36 cm, at 1319.82 mbsf) with high LOI contents are enriched in K, Ba, and Rb. The enrichment of these elements may be ascribed to al-

teration. The patterns of upper dike screen Type 8 metabasalts are in accordance with the patterns of Type 3 to 7 basalt and metabasalts. On the other hand, lower dike screen metabasalts have very low concentrations of REE, Zr, Hf, P, U, and Th (Fig. F5B). The downhole variation of the N-MORB–normalized La/Sm ratio ($La_{[N]}/Sm_{[N]}$) shows that the lower dike screen has notably low $La_{[N]}/Sm_{[N]}$ ratios (0.51–0.57) (Fig. F4G). Gabbros 1 and 2 are characterized by Zr, Hf, and P depletion, except for the high-P_2O_5 sample (312-1256D-221R-1, 61–64 cm; 1440.21 mbsf) with a Zr-, Hf-, U-, and Th-enriched pattern (Fig. F5C). Gabbro 1 has higher $La_{[N]}/Sm_{[N]}$ ratios (0.97–1.42) than Gabbro 2 (0.76–0.90). The Gabbro 1 $La_{[N]}/Sm_{[N]}$ ratio is inversely correlated with REE, Zr, Hf, and P concentrations (Fig. F6).

Mineral compositions

Clinopyroxene

Clinopyroxene Mg# ranges from 64.1 to 86.6. The variation of clinopyroxene Mg# versus TiO_2 shows two domains of high- and low-TiO_2 contents (Fig. F7). Phenocryst, microlite, and microgranular clinopyroxene of basalts and metabasalts show a high-TiO_2 trend, with TiO_2 increasing with decreasing Mg# (Fig. F7A). Amphibole intergrowth–type and secondary-type clinopyroxene of the metabasalts are plotted in the low-TiO_2 (<0.3 wt%) field (Fig. F7A, F7B). Secondary-type clinopyroxenes are found in Type 7 metabasalt, the bottom of Gabbro 1, the upper dike screen, the top of Gabbro 2, and the top of the lower dike screen (Fig. F8A). Igneous-type clinopyroxene of Gabbro 1 shows the high-TiO_2 trend (Fig. F7B). Gabbro 2 igneous-type clinopyroxene also plots on the high-TiO_2 trend, except some clinopyroxenes plot in the low-TiO_2 field of amphibole intergrowth–type plots (Fig. F7B). The compositional range of the igneous-type clinopyroxenes in Gabbros 1 and 2 approximately equals the metabasalt phenocrysts and microlites. Gabbro 2 amphibole-type clinopyroxene has a lower TiO_2 than the igneous-type clinopyroxene of Gabbros 1 and 2. Some amphibole-type clinopyroxenes overlap the secondary-type clinopyroxene. The low-TiO_2 amphibole-type clinopyroxene does not preserve the primary compositions but is of metamorphic origin. Subophitic and coarse-grained network domains in Gabbro 1 clinopyroxenes have different composition. Clinopyroxene oikocryst of subophitic domains have constant Mg# (80.7–82.4). In contrast, coarse-grained network domains show more evolved and variable Mg# (66.3–76.3) than the subophitic domains. Gabbro 1 igneous-type clinopyroxene has negative correlation between TiO_2 and Mg# and the lowest Mg# and the highest TiO_2 occurs in a coarse-grained network domain at the top of the Gabbro 1 subunit (Figs. F7B, F8A, F8B). Gabbro 2 clinopyroxene is slightly evolved toward the top of the Gabbro 2 subunit (Fig. F8A).

Orthopyroxene

Orthopyroxenes show a broad positive correlation between TiO_2 and Mg#, except for some analyses with very low TiO_2 (Fig. F9A). A disseminated oxide olivine gabbro (Sample 312-1256D-215R-2, 56–59 cm; 1417.69 mbsf) of Gabbro 1 includes these exceptionally low TiO_2 orthopyroxenes, which occur as a cluster within an olivine pseudomorph. Gabbro 1 orthopyroxenes have a wider range of Mg# (56.2–75) than those from Gabbro 2 (62.2–73.2). Gabbro 1 orthopyroxene TiO_2 decreases uphole through Gabbro 1 with decreasing Mg# (Fig. F8C). This is opposite behavior from the TiO_2 versus Mg# plots of the clinopyroxene (Figs. F8C, F8D, F9A). These results strongly suggest that the orthopyroxene of Gabbro 1 is of metamorphic origin.

The lowest and highest Mg# orthopyroxenes occur at the top and bottom of Gabbro 2. In the lower part of Gabbro 2, TiO_2 content increases uphole with decreasing Mg#. In contrast, TiO_2 content in the upper part decreases uphole with decreasing Mg# (Figs. F8C, F8D). This suggests the possibility that the orthopyroxene in the lower part of Gabbro 2 is also of metamorphic origin.

Orthopyroxenes of Type 7 and 8 metabasalts have a similar composition to Gabbros 1 and 2 with respect to Mg# and TiO_2. Type 8 metabasalts of the lower dike screen have a slightly higher Mg# than Type 7 metabasalts (Fig. F9A).

Olivine

Olivine decreases in forsterite (Fo) contents with decreasing NiO. Gabbro 2 olivines have slightly lower NiO_2 than those of Gabbro 1 at a given Fo. A sample from the upper part of Gabbro 1 (Sample 312-1256D-215R-1, 20–23 cm; 1415.92 mbsf) has olivine with a much higher Fo content (Fo = 76.6–80.2) than the other Gabbro 1 (Fo = 64.8–70.4) (Fig. F9B). Gabbro 1 olivines usually show normal zoning. In contrast, Gabbro 2 olivines are reversely zoned with Fo contents ranging from 67.3 to 74.5 (Fig. F10).

Plagioclase

Plagioclase ranges in An content from 11 to 83, and most compositions fall within $An_{40–80}$. Very low An content (<An_{40}) is observed in some plagioclase rims

of the upper part of Gabbro 1. These low-An plagioclases (<An_{40}) are not primary magmatic products and may be ascribed to secondary albitization. Plagioclase forms two groups in the An-MgO variation diagram: high- and low-MgO groups. In the high-MgO group, MgO content increases with increasing An%, whereas in the low-MgO group, it does not vary with increasing An% (Fig. F9C, F9D). Plagioclases of the upper and lower dike screen have very low MgO. Most of the plagioclase does not exceed the detection limit of MgO (<0.02 wt%). The laths and phenocrysts of Type 3 basalts belong to the high-MgO group. The MgO content stays almost constant irrespective of An content, except the laths of one low-An sample (312-1256D-176R-1, 21–24 cm; 1276.29 mbsf) (Fig. F9C). The plagioclases of Type 6, 7, and 8 metabasalts belong to the low-MgO group, where the MgO content does not exceed 0.1 wt% over the entire range of An. Gabbro 1 and 2 plagioclases have uniformly low MgO contents over a wide range in An. These plagioclases generally show normal zoning (Fig. F8E).

Acknowledgments

The authors are deeply grateful to Professor Susumu Umino of Kanazawa University and Dr. Jürgen Koepke of Leibniz Universitaet Hannover, whose enormous support and insightful comments were of inestimable value for our study. Samples were provided by the Integrated Ocean Drilling Program (IODP). Shusaku Yamazaki, Natsuki Neo, and Sumio Miyashita were supported by the Center of Deep Earth Exploration (CDEX) for travel fares. S. Yamazaki was supported by the Fellowships of the Japan Society for the Promotion of Science for Young Scientists. The authors are grateful to the Expedition 312 shipboard party and IODP staff.

References

Eggins, S.M., Woodhead, J.D., Kinsley, L.P.J., Mortimer, G.E., Sylvester, P., McCulloch, M.T., Hergt, J.M., and Handler, M.R., 1997. A simple method for the precise determination of ≥40 trace elements in geological samples by ICPMS using enriched isotope internal standardisation. *Chem. Geol.,* 134(4):311–326. **doi:10.1016/S0009-2541(96)00100-3**

Imai, N., Terashima, S., Itoh, S., and Ando, A., 1995. 1994 compilation of analytical data for minor and trace elements in seventeen GSJ geochemical reference samples, "igneous rock series." *Geostand. Geoanal. Res.,* 19(2):135–213. **doi:10.1111/j.1751-908X.1995.tb00158.x**

Koepke, J., Christie, D.M., Dziony, W., Holtz, F., Lattard, D., Maclennan, J., Park, S., Scheibner, B., Yamasaki, T., and Yamazaki, S., 2008. Petrography of the dike–gabbro transition at IODP Site 1256 (equatorial Pacific): the evolution of the granoblastic dikes. *Geochem. Geophys. Geosyst.*, 9(7):Q07O09. **doi:10.1029/2008GC001939**

Roser, B., Kimura, J., and Hisatomi, K., 2000. Whole-rock elemental abundances in sandstones and mudrocks from the Tanabe Group, Kii Peninsula, Japan. *Shimane Diagaku Chikyu Shigen Kankyogaku Kenkyu Hokoku,* 19:101–112.

Sun, S.-S., and McDonough, W.F., 1989. Chemical and isotopic systematics of oceanic basalts: implications for mantle composition and processes. *In* Saunders, A.D., and Norry, M.J. (Eds.), *Magmatism in the Ocean Basins*. Geol. Soc. Spec. Publ., 42(1):313–345. **doi:10.1144/GSL.SP.1989.042.01.19**

Wilson, D.S., Teagle, D.A.H., Alt, J.C., Banerjee, N.R., Umino, S., Miyashita, S., Acton, G.D., Anma, R., Barr, S.R., Belghoul, A., Carlut, J., Christie, D.M., Coggon, R.M., Cooper, K.M., Cordier, C., Crispini, L., Durand, S.R., Einaudi, F., Galli, L., Gao, Y., Geldmacher, J., Gilbert, L.A., Hayman, N.W., Herrero-Bervera, E., Hirano, N., Holter, S., Ingle, S., Jiang, S., Kalberkamp, U. Kerneklian, M., Koepke, J., Laverne, C., Vasquez, H.L.L., Maclennan, J., Morgan, S., Neo, N., Nichols, H.J., Park, S.-H., Reichow, M.K., Sakuyama, T., Sano, T., Sandwell, R., Scheibner, B., Smith-Duque, C.E., Swift, S.A., Tartarotti, P., Tikku, A.A., Tominaga, M., Veloso, E.A., Yamasaki, T., Yamazaki, S., and Ziegler, C., 2006. Drilling to gabbro in intact ocean crust. *Science,* 312(5776):1016–1020. **doi:10.1126/science.1126090**

Initial receipt: 11 September 2008
Acceptance: 2 April 2009
Publication: 21 July 2009
MS 309312-203

Figure F1. Microphotographs of typical rock textures of Gabbros 1 and 2 and lower dike screen. **A.** Boundary between subophitic and coarse-grained network domains in oxide-bearing gabbro (Gabbro 1) (Sample 312-1256D-214R-2, 78–81 cm; 1413.13 mbsf). Network domain has distinct exsolution lamellae. **B.** Same as A (cross-polarized light). Clinopyroxene with exsolution lamellae replaces poikilitic clinopyroxene in subophitic domain. Clinopyroxenes of both domains are igneous-type. Plagioclase in the coarse-grained network domain shows normal zoning. **C.** Disseminated oxide gabbronorite (Gabbro 2), which consists of Fe-Ti oxide, clinopyroxene, orthopyroxene, and plagioclase with cloudy core and clear rim due to numerous submicrometer opaque inclusions (Sample 312-1256D-232R-2, 10–14 cm; 1494.08 mbsf). Both orthopyroxene and clinopyroxene are recrystallized to green and brown amphibole. **D.** Disseminated oxide gabbronorite (Gabbro 2) (Sample 312-1256D-231R-2, 95–98 cm, 1490.14 mbsf). Amphibole intergrowth–type clinopyroxenes are partially replaced by green and brown amphibole and Fe-Ti oxides a few to a few tens of micrometers in diameter. **E.** Area adjacent to D, same thin section. Igneous type clinopyroxene characterized by exsolution lamellae with submicrometer-sized opaque minerals. **F.** Type 8 metabasalt (lower dike screen), showing granular texture like oxide gabbronorite (Sample 312-1256D-233R-1, 4–7 cm; 1497.50 mbsf). Secondary clinopyroxene with very low TiO_2 forms a cluster or vein. Small cluster is visible at the center right. **G.** Type 8 metabasalt (lower dike screen) (Sample 312-1256D-234R-1, 1–2 cm; 1502.50 mbsf). 0.5 to 1.0 mm size euhedral plagioclase laths and relict clinopyroxene are embedded in the matrix of microgranular secondary clinopyroxene, orthopyroxene, plagioclase and Fe-Ti oxides. Plagioclase lath has granular opaque and transparent inclusions a few micrometers in diameter. **H.** Same as G (cross-polarized light). pl = plagioclase, cpx = clinopyroxene, amp = amphibole, ox = Fe-Ti oxide, opx = orthopyroxene. (**Figure shown on next page.**)

Figure F1 (continued). (Caption shown on previous page.)

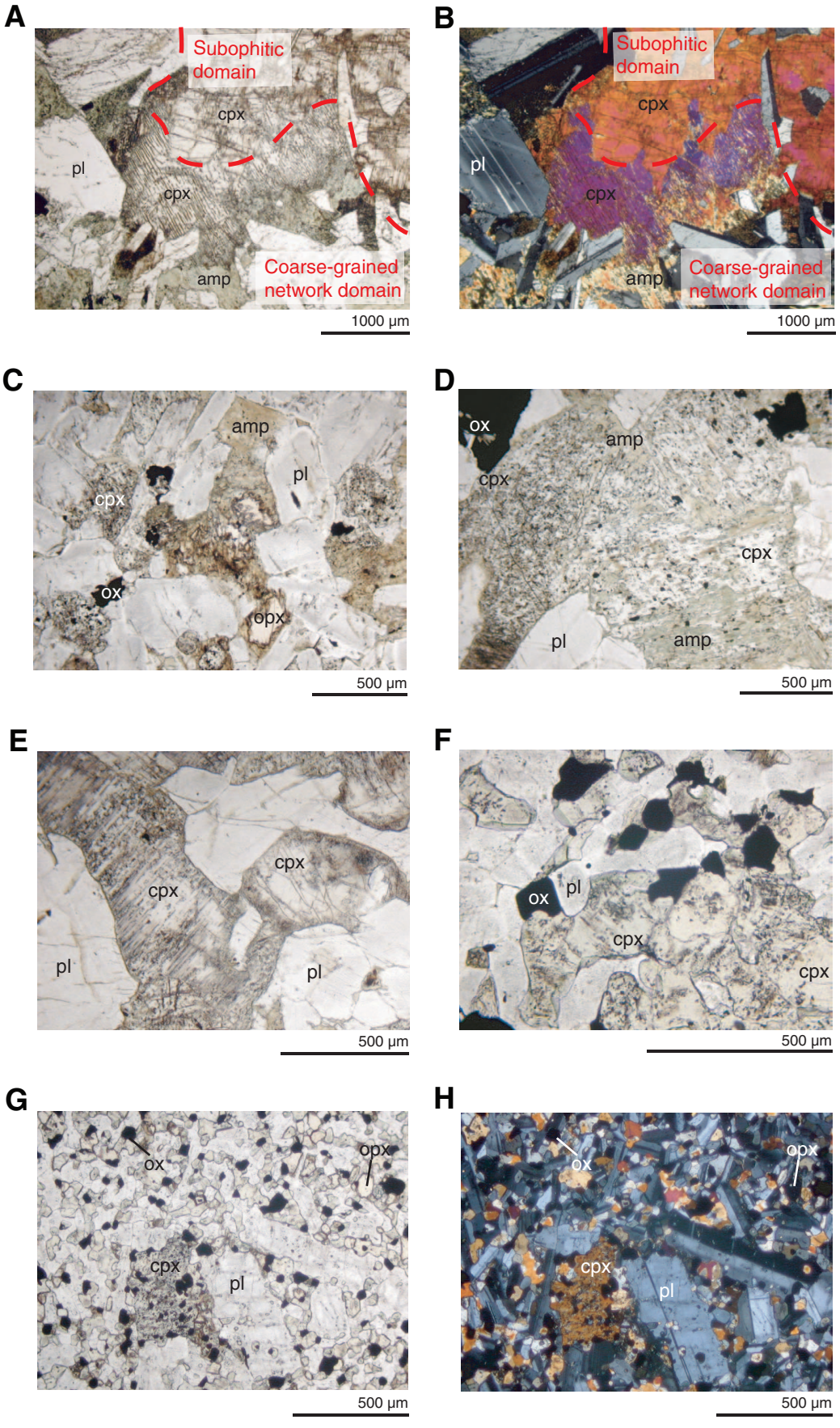

Figure F2. Images of typical heterogeneous texture of upper part of Gabbro 1, which is characterized by two textual domains: subophitic and coarse-grained patchy or network. **A.** Scan image of wet surface of oxide gabbro (Sample 312-1256D-214R-2, 78–81 cm; 1413.13 mbsf). White brackets = area of thin section in B and C. **B.** Thin section image of A (cross-polarized light). Subophitic domains are characterized by <1 cm clinopyroxene oikocrysts with plagioclase chadocrysts. Coarse-grained network domains are characterized by plagioclase and Fe-Ti oxide. **C.** Thin section image of A (plane-polarized light). Red dashed line = boundary between coarse-grained network domain and subophitic domain. Yellow box = area of the photomicrographs in Figure F1A and F1B.

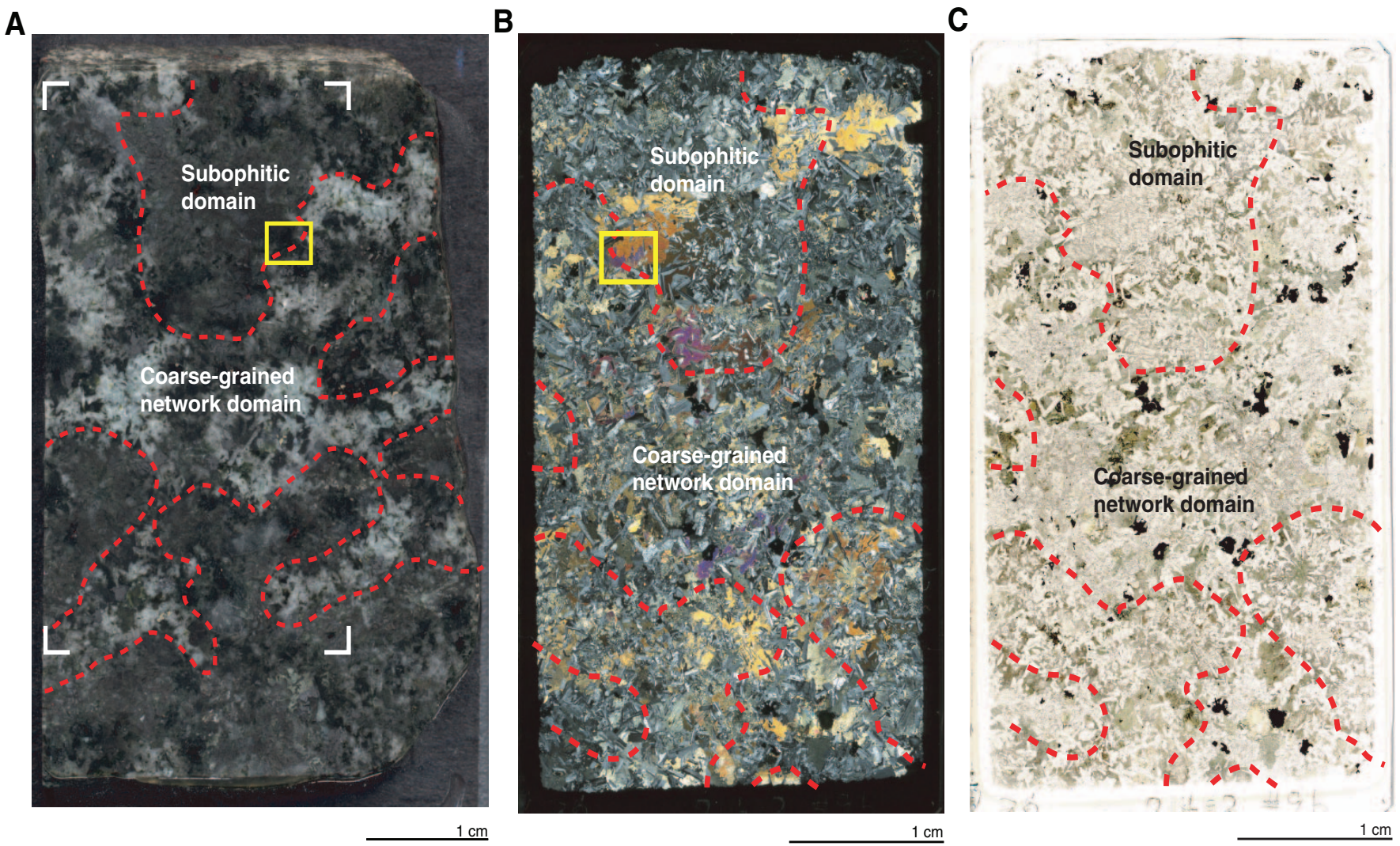

Figure F3. Variation diagrams of whole-rock compositions. **A.** SiO_2 vs. Mg# (100 × Mg/[Mg + Fe]). **B.** Loss on ignition vs. K_2O. **C.** Mg# vs. TiO_2. **D.** Mg# vs. P_2O_5.

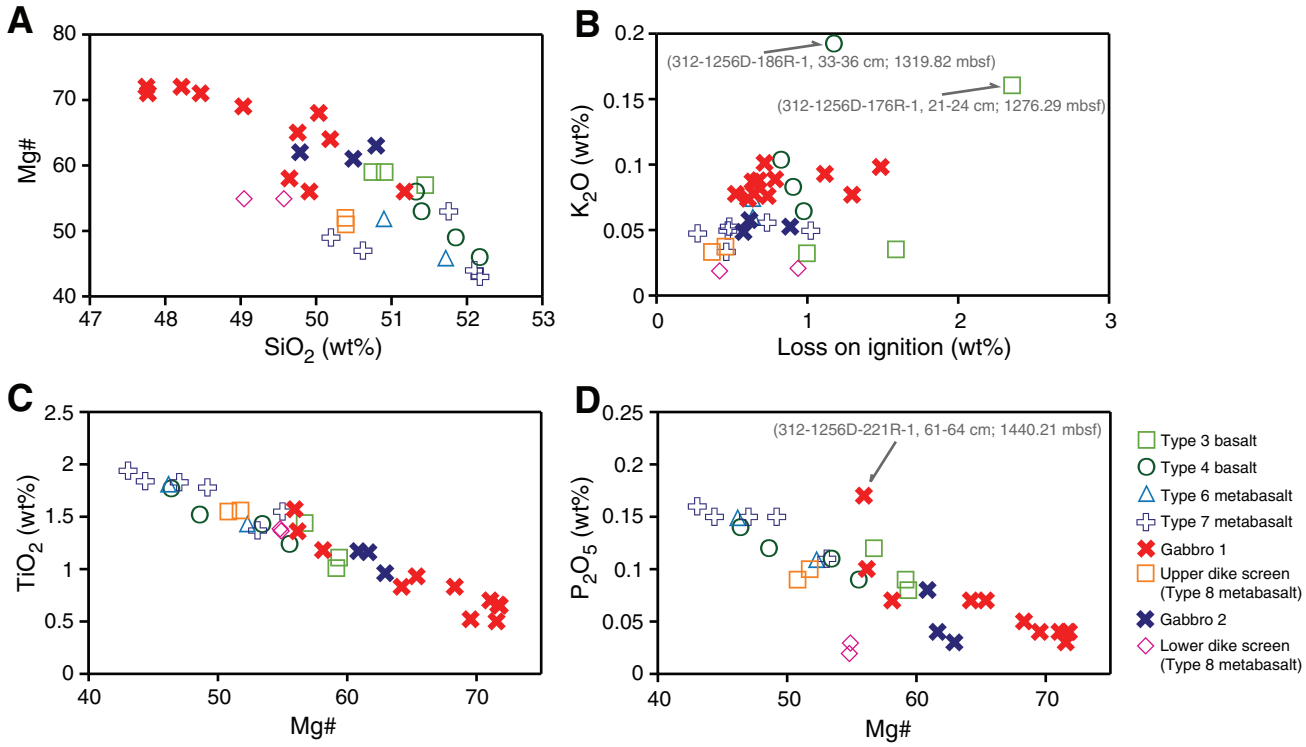

Figure F4. Downhole variation diagrams of (**A**) SiO_2, (**B**) Mg#, (**C**) TiO_2, (**D**) P_2O_5, (**E**) Zr, (**F**) Zr/Y ratio, and (**G**) La/Sm ratio normalized to normal mid-ocean-ridge basalt values of Sun and McDonough (1989).

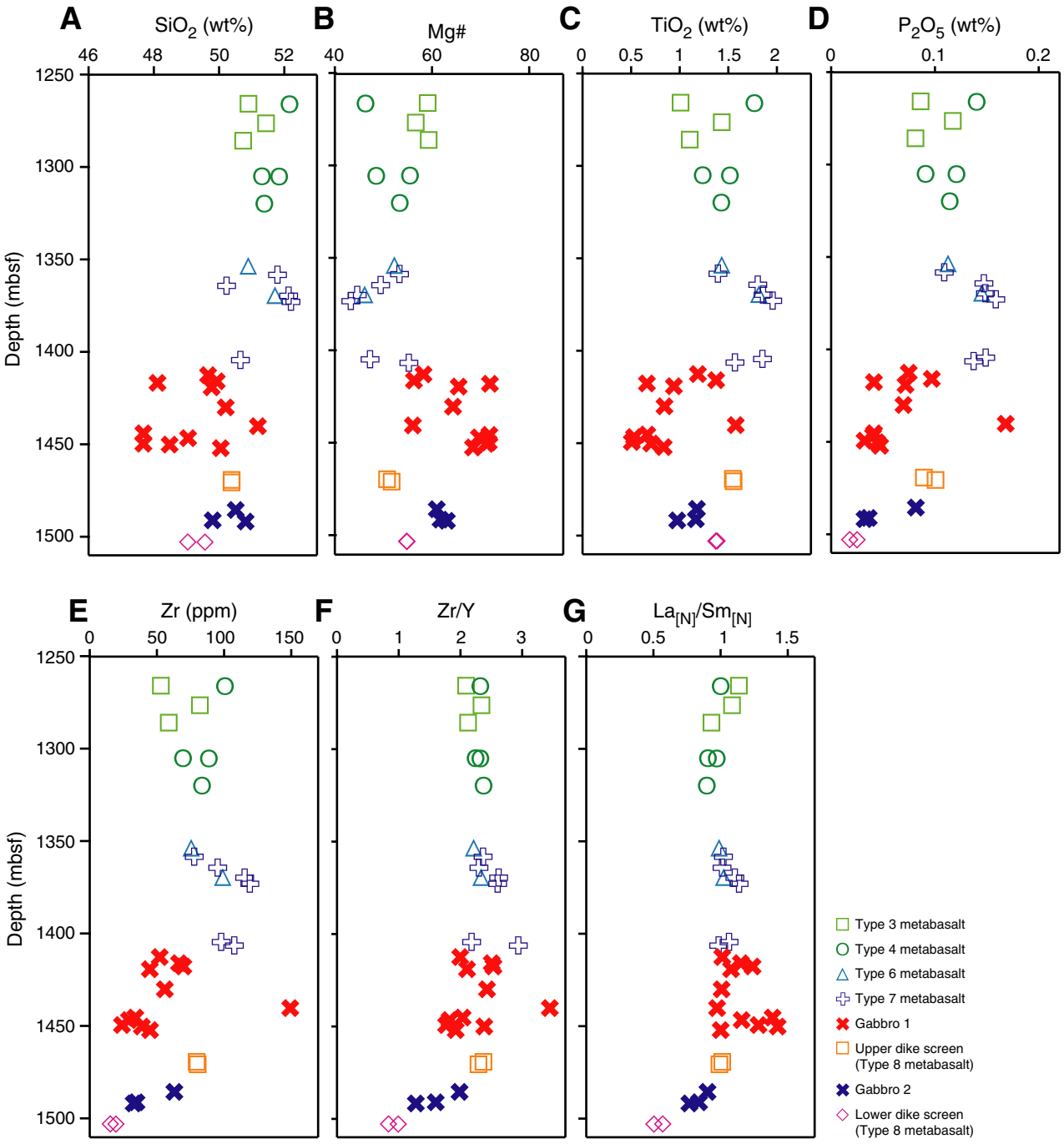

Figure F5. Trace element patterns normalized to normal mid-ocean-ridge basalt (N-MORB) values of Sun and McDonough (1989). **A.** Type 3 and 4 basalts and Type 6 and 7 metabasalts. **B.** Gabbro 1. **C.** Gabbro 2. **D.** Upper and lower dike screen (Type 8 metabasalts). Numeric value of symbol indicates sampling depth (meters below seafloor).

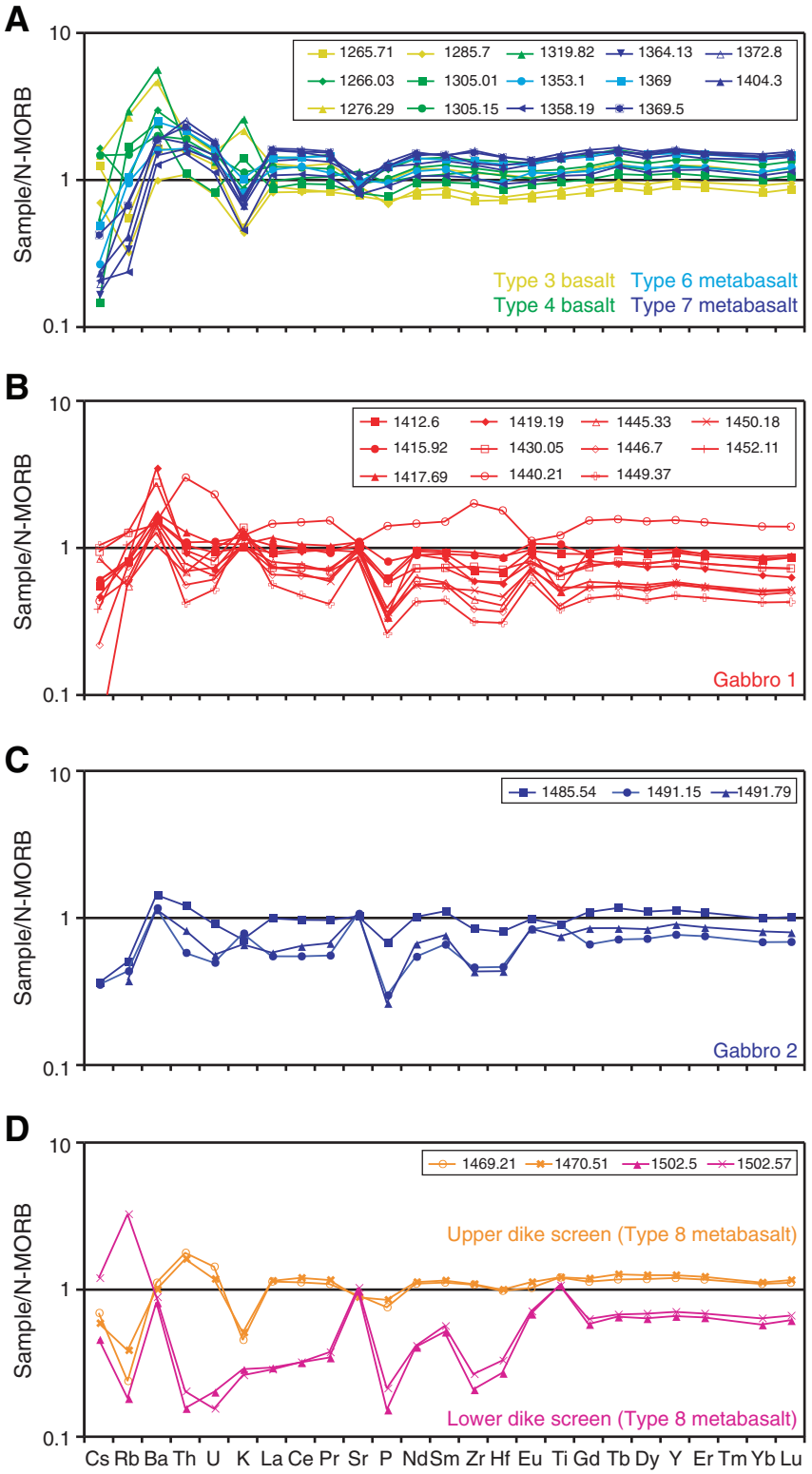

Figure F6. Normal mid-ocean-ridge basalt–normalized La/Sm ratio plotted against Zr.

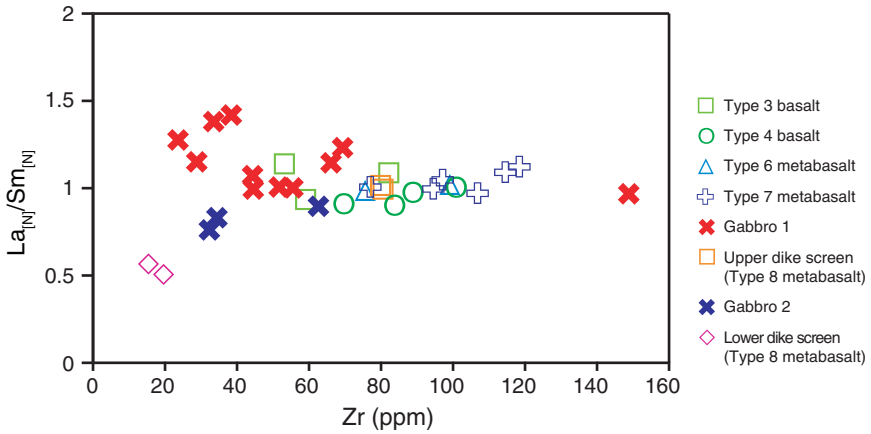

Figure F7. Variation diagrams showing clinopyroxene Mg# vs. TiO_2 for (**A**) Type 3 to 7 basalts and metabasalts and the upper and lower dike screen, (**B**) Gabbros 1 and 2, and (**C**) subophitic and coarse-grained network domains of Gabbro 1.

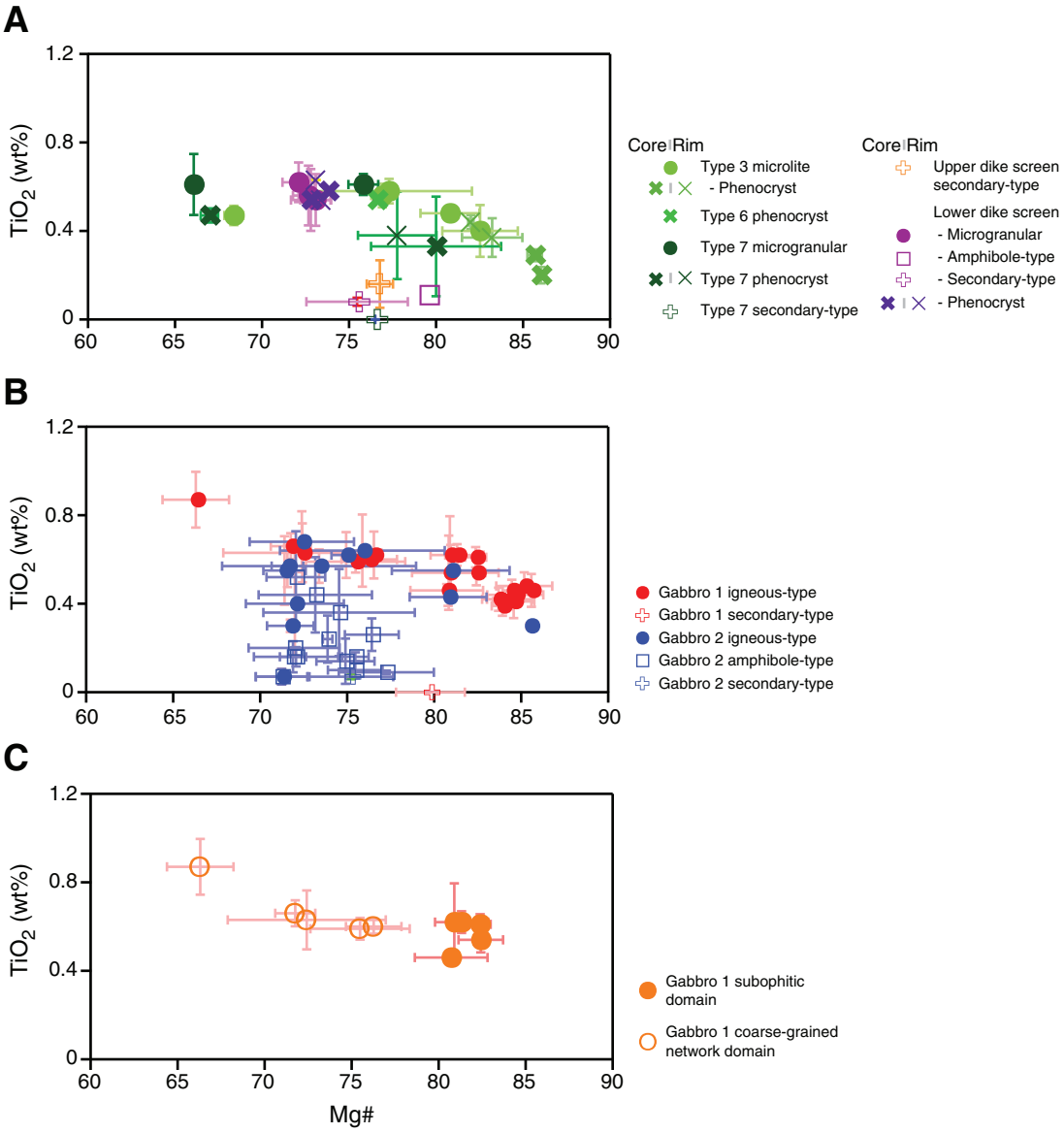

Figure F8. Downhole variations showing clinopyroxene (Cpx) (**A**) Mg# (**B**) and TiO_2, orthopyroxene (Opx) (**C**) Mg# and (**D**) TiO_2, plagioclase (Pl) (**E**) anorthite (An) and (**F**) MgO, and (**G**) olivine (Ol) forsterite (Fo). Lower depth range = close-up of Gabbro 2 and lower dike screen. Green sections = basalts, blue sections = gabbros, gray spotted pattern = granoblastic dikes. Symbols for plagioclase, orthopyroxene, and olivine are the same as in Figure F9. Symbols for clinopyroxene are the same as in Figure F7.

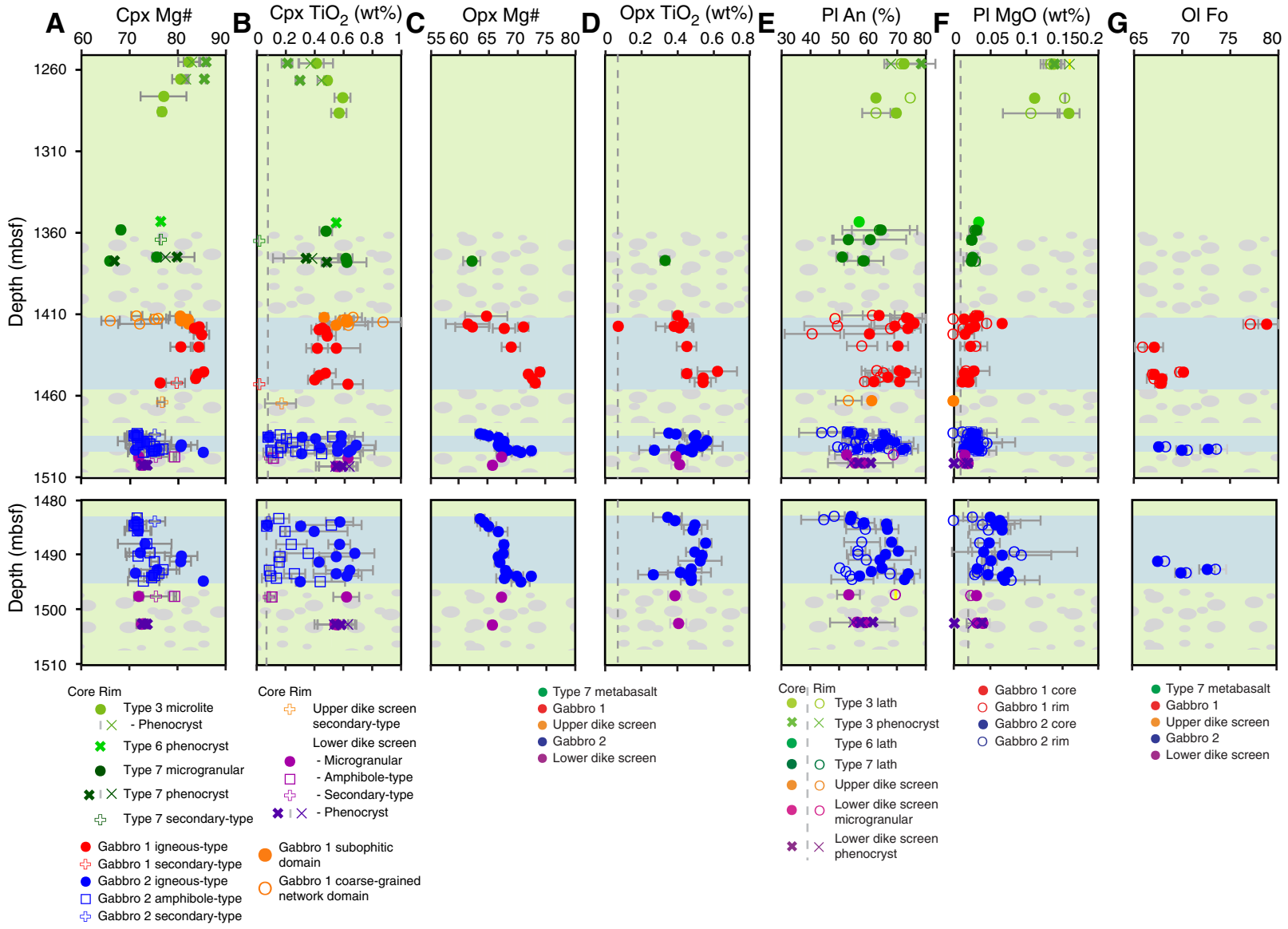

Figure F9. Mineral compositions of (**A**) orthopyroxene Mg# vs. TiO_2, (**B**) olivine forsterite (Fo) vs. NiO, and plagioclase anorthite (An) vs. (**C**) MgO of Type 3 to 8 basalts and metabasalts and (**D**) Gabbros 1 and 2.

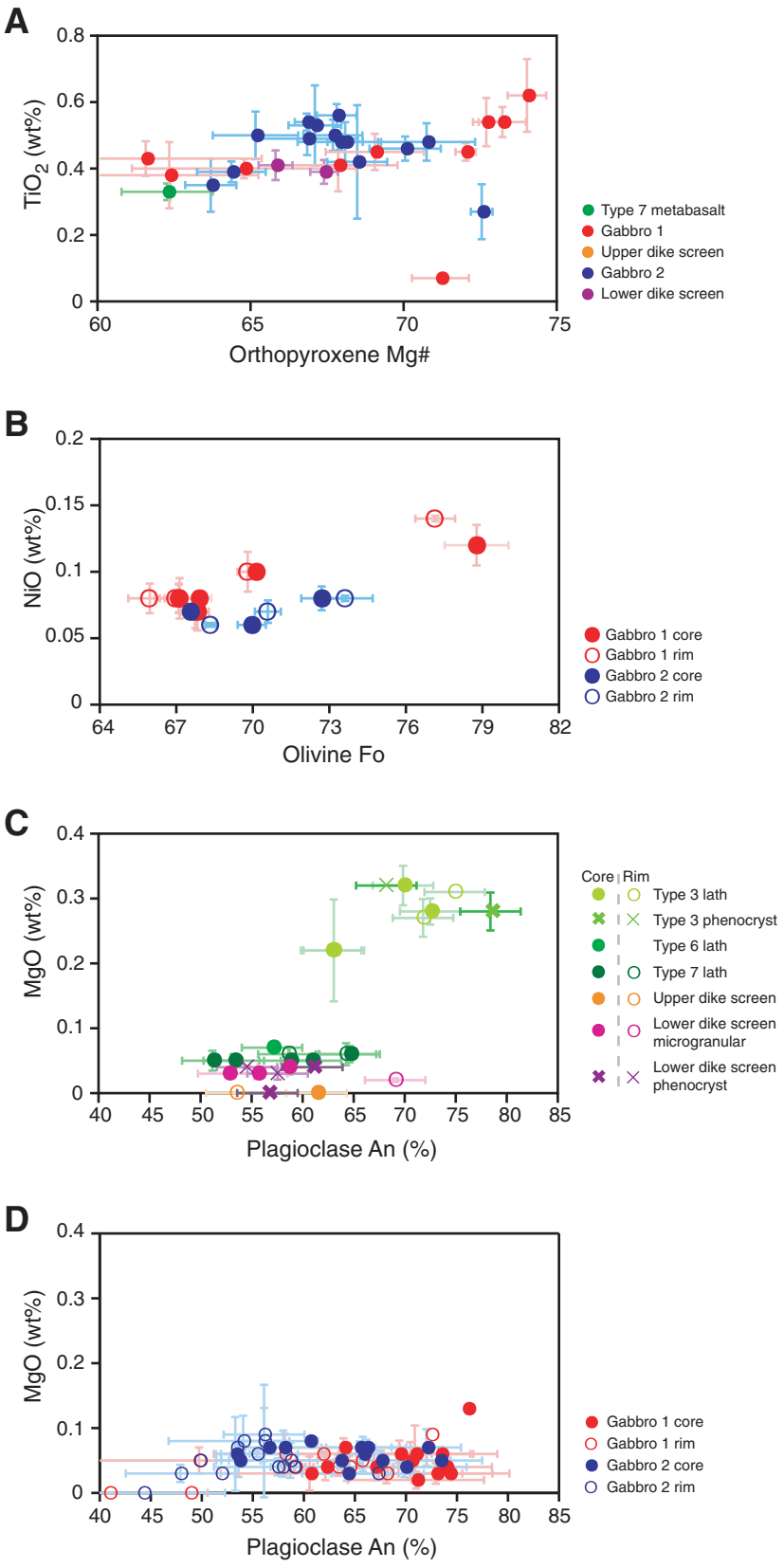

Figure F10. Olivine forsterite (Fo) content of core vs. rim. Gabbro 1 olivines plotted below the line are normally zoned; Gabbro 2 olivines are reversely zoned and plot above the line.

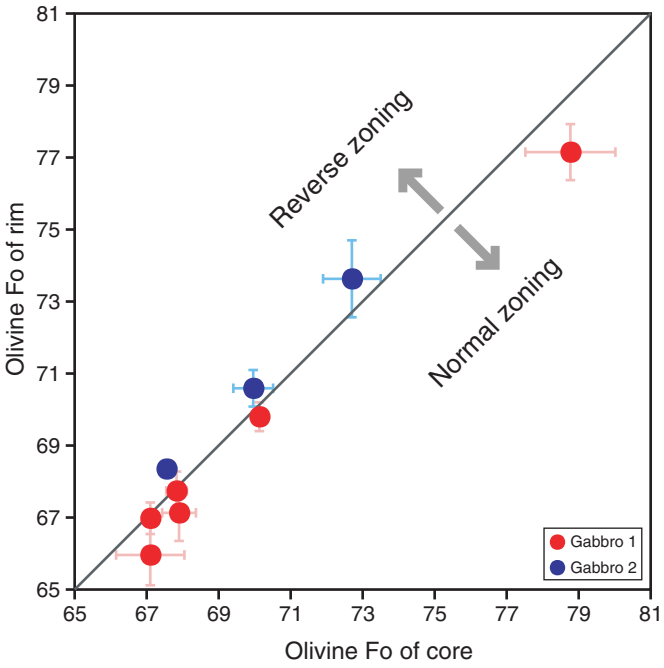

Table T1. Analyzed samples, Hole 1256D. (See table notes.) (Continued on next page.)

Core, section, interval (cm)	Depth (mbsf)	Unit	Lithology	Rock name and basalt texture type	Phenocryst assemblages for basalt	Igneous mineral assemblages for gabbro	Secondary mineral assemblage	XRF and ICP-MS	
								EPMA	
312-1256D-									
172R-1,12–14	1255.20	66	Sheeted dike	Type 3 basalt	Pl, Cpx		DBM, Chl	X	
174R-1, 32–34	1265.71	68	Sheeted dike	Type 3 basalt	Pl, Cpx		DBM, Chl	X	X
174R-1, 64–67	1266.03	68	Sheeted dike	Type 4 basalt	Aphyric		DBM, Chl		X
176R-1, 21–24	1276.29	69	Sheeted dike	Type 3 basalt	Pl, Cpx		DBM, Chl	X	X
178R-1, 0–3	1285.70	73	Sheeted dike	Type 3 basalt	Pl		DBM, Chl	X	X
182R-1, 12–15	1305.01	73	Sheeted dike	Type 4 basalt	Aphyric		DBM, Chl, Ox		X
184R-1, 39–41	1305.15	74	Sheeted dike	Type 4 basalt	Pl, Cpx		DBM, Chl, Ox		X
186R-1, 33–36	1319.82	75A	Sheeted dike	Type 4 basalt	Aphyric		DBM, Chl, Ox, Amp		X
193R-1, 5–8	1353.10	78	Granoblastic dike	Type 6 metabasalt	Aphyric		DBM, Ox, Amp	X	X
194R-1, 29–33	1358.19	78	Granoblastic dike	Type 7 metabasalt	Pl		DBM, Ox, Amp, Opx	X	X
196R-1, 43–46	1364.13	78	Granoblastic dike	Type 7 metabasalt	Pl		Chl, Ox, Amp, Cpx, Opx	X	X
198R-1, 0–5	1369.00	78	Granoblastic dike	Type 6 metabasalt	Aphyric		DBM, Ox, Amp		X
198R-1, 50–54	1369.50	78	Granoblastic dike	Type 7 metabasalt	Aphyric		DBM, Chl, Ox, Amp, Cpx, Opx		X
202R-1, 5–8	1372.80	79	Granoblastic dike	Type 7 metabasalt	Aphyric		DBM, Ox, Amp, Cpx, Opx		X
203R-1, 6–10	1374.89	80A	Granoblastic dike	Type 7 metabasalt	Pl, Cpx		Amp, Ox, Cpx, Opx, Qtz	X	
204R-1, 0–4	1377.30	80A	Granoblastic dike	Type 7 metabasalt	Aphyric		Amp, Ox, Cpx, Opx	X	
212R-1, 20–23	1404.30	80A	Granoblastic dike	Type 7 metabasalt	Aphyric		Chl, Amp, Ox, Cpx, Opx		X
214R-1, 19–21	1411.10	81	Gabbro 1	Opx-bearing ol gabbro		Pl, Cpx, Ol, Opx, Ox	Amp, Tlc, Id	X	
214R-2, 24–27	1412.60	83	Gabbro 1	Disseminated oxide gabbro		Pl, Cpx, Ox	Chl, Amp, Ox	X	X
214R-2, 78–81	1413.13	85	Gabbro 1	Disseminated oxide gabbro		Pl, Cpx, Ol, Ox	Chl, Amp, Ox, Ep, Id	X	
214R-3, 18–21	1413.99	85	Gabbro 1	Disseminated oxide ol gabbro		Pl, Cpx, Ox	Amp, Ox, Id, Ab	X	
215R-1, 20–23	1415.92	85	Gabbro 1	Disseminated oxide ol gabbro		Pl, Cpx, Ol, Opx, Ox	Amp, Chl, Ox, Ep, Id, Ab	X	X
215R-2, 56–59	1417.69	86A	Gabbro 1	Disseminated oxide ol gabbro		Pl, Cpx, Ox	Amp, Ox, Id, Ab	X	X
216R-1, 72–75	1418.62	86A	Gabbro 1	Ol gabbro		Pl, Cpx	Amp, Ox, Id, Tlc	X	
216R-1, 138–142	1419.19	86	Gabbro 1	Ol gabbro		Pl, Cpx	Chl, Amp, Ox	X	X
217R-1, 94–97	1422.54	88	Gabbro 1	Gabbro		Pl, Cpx	Amp, Ox, Id, Ab	X	
218R-1, 1–3	1430.00	88	Gabbro 1	Gabbro		Pl, Cpx	Amp, Ox, Cal, Zeo, Ant, Ab	X	
219R-1, 5–8	1430.05	88	Gabbro 1	Opx-bearing ol gabbro		Pl, Cpx, Ol, Opx	Amp, Ox, Id	X	X
221R-1, 61–64	1440.21	88	Gabbro 1	Opx-bearing gabbro		Pl, Cpx	Amp, Ox, Ab		X
222R-1, 73–78	1445.33	88	Gabbro 1	Opx-bearing ol gabbro		Pl, Cpx, Ol	Amp, Ox, Id, Tlc	X	X
222R-2, 60–63	1446.70	88	Gabbro 1	Opx-bearing ol gabbro		Pl, Cpx, Ol, Opx	Amp, Ox, Id	X	X
223R-1, 8–12	1449.37	88	Gabbro 1	Opx-bearing ol gabbro		Pl, Cpx, Ol, Opx	Amp, Ox, Id, Cal	X	X
223R-1, 88–91	1450.18	88	Gabbro 1	Opx-bearing ol gabbro		Pl, Cpx, Ol, Opx	Amp, Ox, Id, Tlc		X
223R-2, 133–137	1452.11	89A	Gabbro 1	Ol gabbronorite		Pl, Cpx, Ol, Opx, Ox	Amp, Ox	X	X
226R-1, 0–4	1463.90	90A	Upper dike screen	Type 8 metabasalt	Aphyric		Amp, Ox, Cpx, Opx	X	
227R-1, 72–76	1469.21	90A	Upper dike screen	Type 8 metabasalt	Aphyric		Amp, Ox, Cpx, Opx		X
227R-2, 50–59	1470.51	90A	Upper dike screen	Type 8 metabasalt	Aphyric		Amp, Ox, Cpx, Opx		X
230R-1, 19–21	1483.19	90A	Gabbro 2	Disseminated oxide opx-bearing gabbro		Pl, Cpx, Opx, Ox	Amp, Ox	X	
230R-1, 81–84	1483.81	91A	Gabbro 2	Disseminated oxide gabbro		Pl, Cpx, Opx, Ox	Amp, Ox	X	
230R-1, 139–142	1484.38	92A	Gabbro 2	Gabbronorite		Pl, Cpx, Opx	Amp, Ox	X	
230R-2, 32–36	1484.58	92A	Gabbro 2	Gabbronorite		Pl, Cpx, Opx	Amp, Ox	X	
230R-2, 104–109	1485.54	92A	Gabbro 2	Gabbronorite		Pl, Cpx, Opx, Ox	Amp, Ox	X	X
231R-1, 19–22	1487.90	92A	Gabbro 2	Disseminated oxide gabbronorite		Pl, Cpx, Opx, Ox	Amp, Ox	X	
231R-2, 35–39	1489.54	92A	Gabbro 2	Disseminated oxide gabbronorite		Pl, Cpx, Opx, Ox	Amp, Ox	X	
231R-2, 95–98	1490.14	92A	Gabbro 2	Disseminated oxide gabbronorite		Pl, Cpx, Opx, Ox	Amp, Ox, Id	X	
231R-3, 59–63	1491.15	92A	Gabbro 2	Disseminated oxide ol-bearing gabbronorite		Pl, Cpx, Ol, Opx, Ox	Amp, Ox, Id, Tlc	X	X
231R-3, 123–127	1491.79	92A	Gabbro 2	Disseminated oxide gabbronorite		Pl, Cpx, Opx, Ox	Amp, Ox, Id, Tlc		X

Table T1 (continued).

Core, section, interval (cm)	Depth (mbsf)	Unit	Lithology	Rock name and basalt texture type	Phenocryst assemblages for basalt	Igneous mineral assemblages for gabbro	Secondary mineral assemblage	XRF and ICP-MS	
								EPMA	
231R-4, 70-74	1492.63	92A	Gabbro 2	Opx-bearing ol gabbro		Pl, Cpx, Ol, Opx, Ox	Amp, Ox, Id, Tlc	X	
231R-4, 137-141	1493.30	92A	Gabbro 2	Ol gabbronorite		Pl, Cpx, Opx, Ox	Amp, Ox		
232R-1, 36-39	1493.26	92A	Gabbro 2	Disseminated oxide gabbronorite		Pl, Cpx, Ol, Opx, Ox	Amp, Ox, Id, Tlc	X	
232R-1, 78-82	1493.68	92A	Gabbro 2	Disseminated oxide gabbronorite		Pl, Cpx, Opx, Ox	Amp, Ox, Id	X	
232R-2, 10-14	1494.08	92A	Gabbro 2	Disseminated oxide gabbronorite		Pl, Cpx, Opx, Ox	Amp, Ox, Id	X	
232R-2, 73-76	1494.71	93	Gabbro 2	Disseminated oxide ol gabbronorite		Pl, Cpx, Opx, Ox	Amp, Ox, Id	X	
233R-1, 4-7	1497.50	94	Lower dike screen	Type 8 metabasalt	Cpx		Cpx, Opx, Pl, Ox, Amp	X	
234R-1, 1-2	1502.50	94	Lower dike screen	Type 8 metabasalt	Pl		Cpx, Opx, Pl, Ox, Amp	X	X
234R-1, 7-9	1502.57	94	Lower dike screen	Type 8 metabasalt	Pl		Cpx, Opx, Pl, Ox, Amp	X	X

Notes: For basalt texure type, basalt is classified according to Koepke et al. (2008) and the "Site 1256" chapter. EPMA = JXA-8600SX EPMA at the Graduate School of Science and Technology, Niigata University. XRF = X-ray fluorescence, ICP-MS = inductively coupled plasma–mass spectrometry. Opx = orthopyroxene, Ol = olivine, Pl = plagioclase, Cpx = clinopyroxene, Ox = Fe-Ti oxide, DBM = dusty brown material, Chl = chlorite, Amp = amphibole, Qtz = quartz, Tlc = talc, Id = iddingsite, Ep = epidote, Ab = albite, Zeo = zeolite, Ant = anthophyllite, Cal = calcite.

Table T2. Whole-rock major and trace elements, Hole 1256D. (See table notes.) (Continued on next two pages.)

Core, section:				174R-1	174R-1	176R-1	178R-1	182R-1	184R-1	186R-1	193R-1	194R-1	196R-1	198R-1	198R-1	202R-1	212R-1
Interval (cm):				32–34	64–67	21–24	0–3	12–15	39–41	33–36	5–8	29–33	43–46	0–5	50–54	5–8	20–23
Depth (mbsf):				1265.71	1266.03	1276.29	1285.70	1305.01	1305.15	1319.82	1353.10	1358.19	1364.13	1369.00	1369.50	1372.80	1404.30
Lithology:				SD	SD	SD	SD	SD	SD	SD	GD	GD	GD	GD	GD	GD	GD
Rock name	Reference value	Average (N = 4)	Standard deviation	Type 3 basalt	Type 4 basalt	Type 3 basalt	Type 3 basalt	Type 4 basalt	Type 4 basalt	Type 4 basalt	Type 6 metabasalt	Type 7 metabasalt	Type 7 metabasalt	Type 6 metabasalt	Type 7 metabasalt	Type 7 metabasalt	Type 7 metabasalt
Major element oxide (wt%):																	
SiO_2	53.71	53.77	0.15	50.91	52.18	51.45	50.75	51.33	51.86	51.41	50.90	51.73	50.17	51.72	52.07	52.15	50.60
TiO_2	1.20	1.20	0.00	1.00	1.77	1.42	1.10	1.24	1.51	1.43	1.44	1.37	1.79	1.81	1.83	1.94	1.83
Al_2O_3	14.77	14.77	0.03	14.46	13.09	13.19	14.40	13.94	13.26	13.48	13.31	13.77	13.51	13.10	13.18	12.95	13.23
FeO^{total}	12.95	12.92	0.01	10.02	13.46	10.97	10.03	11.35	12.88	11.93	12.81	11.68	13.50	13.72	14.01	14.26	13.97
MnO	0.22	0.22	0.00	0.22	0.28	0.30	0.18	0.22	0.22	0.20	0.18	0.19	0.18	0.23	0.23	0.23	0.18
MgO	4.66	4.63	0.06	8.15	6.55	8.07	8.24	7.97	6.84	7.70	7.88	7.36	7.29	6.61	6.23	6.01	6.91
CaO	9.91	9.91	0.04	12.08	10.04	11.24	12.22	11.29	10.06	9.76	10.45	11.16	10.73	9.77	9.55	9.77	9.83
Na_2O	2.06	2.02	0.01	1.82	2.39	2.24	2.22	2.25	2.56	3.20	2.82	2.33	2.89	2.69	2.24	2.41	2.91
K_2O	0.43	0.43	0.01	0.03	0.06	0.16	0.03	0.10	0.08	0.19	0.06	0.03	0.05	0.07	0.06	0.05	0.05
P_2O_5	0.10	0.10	0.00	0.09	0.14	0.12	0.08	0.09	0.12	0.11	0.11	0.11	0.15	0.15	0.15	0.16	0.15
LOI				1.59	0.98	2.36	1.00	0.83	0.91	1.18	0.64	0.45	0.26	0.64	0.72	0.47	0.46
Total:	100.00	99.97		100.38	100.94	101.52	100.25	100.62	100.31	100.58	100.61	100.18	100.53	100.51	100.27	100.41	100.10
Mg#:				59.2	46.4	56.7	59.4	55.6	48.6	53.5	52.3	52.9	49.0	46.2	44.2	42.9	46.9
Trace element (ppm):																	
Sc	36.20	35.23	2.94	45.23	47.25	47.68	44.63	43.22	45.01	46.44	42.45	43.29	46.91	45.43	47.14	46.07	48.99
V	270.0	262.3	17.4	280.4	413.0	345.1	304.6	335.7	382.8	389.6	345.4	336.1	429.1	418.4	420.6	449.2	456.8
Ga	17.40	17.46	0.94	14.98	18.24	15.10	15.68	15.64	17.64	16.17	15.95	16.25	18.14	17.75	18.04	18.23	19.64
Rb	20.10	20.65	0.25	0.31	0.54	1.50	0.18	0.94	0.83	1.65	0.53	0.13	0.19	0.59	0.37	0.39	0.23
Sr	191.8	194.5	3.5	70.4	84.6	86.8	83.1	73.5	83.6	103.2	90.7	71.4	95.9	86.5	76.3	79.0	96.8
Y	22.80	23.08	0.58	25.4	43.4	35.1	27.8	31.0	38.2	35.2	34.1	32.7	41.4	42.4	44.0	45.8	44.9
Zr	92.00	98.13	2.58	53.3	101.1	82.3	59.2	69.9	89.1	84.0	75.7	76.4	93.9	99.2	113.9	117.8	96.5
Cs	0.916	0.913	0.017	0.009	0.012	0.010	0.005	0.001	0.010	0.004	0.002	0.001	0.001	0.003	0.003	0.001	0.002
Ba	171.0	174.7	2.81	10.31	18.81	29.52	6.26	15.19	12.57	35.72	10.03	7.97	9.24	15.73	11.78	11.39	12.29
La	10.59	10.88	0.22	2.27	3.57	3.23	2.06	2.20	3.08	2.46	2.93	2.69	3.37	3.52	4.03	4.10	3.97
Ce	23.08	23.60	0.31	6.46	10.64	9.29	6.22	7.08	9.11	7.74	9.25	8.18	10.37	10.69	11.70	12.14	11.61
Pr	3.03	3.07	0.04	1.10	1.96	1.70	1.10	1.23	1.57	1.39	1.48	1.40	1.75	1.91	2.03	2.07	1.90
Nd	12.95	13.25	0.39	5.78	10.17	8.67	6.19	7.01	8.83	7.69	8.36	7.75	9.34	10.26	11.01	11.30	10.68
Sm	3.31	3.37	0.08	2.09	3.74	3.12	2.32	2.54	3.32	2.87	3.11	2.81	3.56	3.62	3.88	3.84	3.98
Eu	1.09	1.13	0.04	0.77	1.33	1.06	0.82	0.95	1.17	1.05	1.14	0.99	1.30	1.30	1.39	1.39	1.36
Gd	3.69	3.74	0.10	3.02	5.47	4.42	3.40	3.71	4.55	4.26	4.22	3.98	5.30	5.29	5.59	5.89	5.65
Tb	0.62	0.62	0.02	0.59	1.08	0.87	0.65	0.74	0.91	0.84	0.85	0.82	1.03	1.05	1.06	1.11	1.04
Dy	3.79	3.84	0.10	3.83	6.73	5.41	4.27	4.91	5.90	5.35	5.51	5.13	6.37	6.77	6.69	7.04	6.88
Ho	0.80	0.82	0.03	0.83	1.51	1.22	0.97	1.05	1.30	1.18	1.20	1.14	1.44	1.50	1.53	1.61	1.59
Er	2.26	2.29	0.07	2.63	4.52	3.70	2.86	3.19	4.07	3.61	3.60	3.49	4.17	4.43	4.44	4.61	4.59
Yb	2.03	2.07	0.05	2.49	4.35	3.43	2.80	3.06	3.84	3.45	3.44	3.27	4.19	4.28	4.36	4.58	4.41
Lu	0.30	0.31	0.01	0.39	0.68	0.55	0.43	0.48	0.61	0.55	0.55	0.52	0.65	0.67	0.69	0.71	0.66
Hf	2.30	2.45	0.06	1.49	2.75	2.23	1.56	1.77	2.33	2.20	1.97	1.92	2.40	2.63	2.93	2.96	2.57
Th	2.21	2.28	0.07	0.19	0.26	0.25	0.13	0.13	0.23	0.21	0.20	0.18	0.19	0.26	0.28	0.31	0.21
U	0.50	0.50	0.01	0.06	0.07	0.07	0.04	0.04	0.07	0.06	0.07	0.05	0.06	0.08	0.08	0.09	0.07

Notes: SD = sheeted dike, GD = granoblastic dike, G1 = Gabbro 1, UDS = upper dike screen, G2 = Gabbro 2, LDS = lower dike screen. Major element oxide based on JB-2 reference values from Imai et al. (1995), trace elements based on W-2 reference values from Eggins et al. (1997). FeO^{total} = total Fe as FeO.

Table T2 (continued). (Continued on next page.)

Core, section:	214R-2	215R-1	215R-2	216R-1	219R-1	221R-1	222R-1	222R-2	223R-1	223R-1	223R-2	227R-1	227R-2
Interval (cm):	24–27	20–23	56–59	138–142	5–8	61–64	73–78	60–63	8–12	88–91	133–137	72–76	50–59
Depth (mbsf):	1412.60	1415.92	1417.69	1419.19	1430.05	1440.21	1445.33	1446.70	1449.37	1450.18	1452.11	1469.21	1470.51
Lithology:	G1	G1	G1	G1	G1	G1	G1	G1	G1	G1	G1	UDS	UDS
Rock name	Disseminated oxide gabbro	Disseminated oxide olivine gabbro	Disseminated oxide olivine gabbro	Olivine gabbro	Orthopyroxene-bearing olivine gabbro	Orthopyroxene-bearing olivine	Orthopyroxene-bearing olivine gabbro	Olivine gabbro	Orthopyroxene-bearing olivine gabbro	Orthopyroxene-bearing olivine gabbro	Olivine gabbronorite	Type 8 metabasalt	Type 8 metabasalt
Major element oxide (wt%):													
SiO_2	49.63	49.90	48.20	49.74	50.17	51.16	47.74	49.02	47.76	48.46	50.02	50.40	50.40
TiO_2	1.17	1.36	0.65	0.92	0.83	1.56	0.65	0.51	0.49	0.69	0.82	1.55	1.56
Al_2O_3	15.84	16.10	14.27	15.76	15.35	14.99	14.15	15.89	14.7	15.7	14.63	13.57	13.74
FeO^{total}	9.71	9.83	9.03	8.06	8.54	10.13	8.99	7.81	8.59	8.09	8.46	13.06	12.32
MnO	0.14	0.14	0.13	0.13	0.15	0.17	0.13	0.12	0.13	0.12	0.15	0.22	0.17
MgO	7.54	7.05	12.85	8.50	8.57	7.20	12.72	9.96	12.07	11.11	10.20	7.58	7.42
CaO	12.61	11.89	12.07	13.50	12.99	11.00	12.01	13.20	12.64	12.36	13.14	11.23	11.49
Na_2O	2.55	2.92	2.16	2.42	2.30	3.12	2.07	2.30	1.90	2.27	2.23	2.47	2.66
K_2O	0.07	0.09	0.08	0.09	0.10	0.09	0.08	0.08	0.10	0.09	0.08	0.03	0.04
P_2O_5	0.07	0.10	0.04	0.07	0.07	0.17	0.04	0.04	0.03	0.04	0.05	0.09	0.10
LOI	0.60	0.63	0.64	0.67	0.71	0.78	1.29	0.73	1.48	1.11	0.52	0.37	0.46
Total:	99.93	100.00	100.12	99.85	99.77	100.36	99.86	99.66	99.89	100.04	100.30	100.57	100.37
Mg#:	58.1	56.1	71.7	65.3	64.1	55.9	71.5	69.5	71.5	71.0	68.2	50.8	51.8
Trace element (ppm):													
Sc	41.77	40.09	42.59	40.66	44.46	41.94	38.40	38.21	38.19	32.91	46.54	46.91	46.23
V	272.8	287.4	310.5	240.9	232.9	429.3	213.7	179.2	171.2	170.1	254.3	461.1	412.7
Ga	15.38	16.49	16.04	13.61	14.78	19.49	12.74	13.69	12.92	13.43	14.74	17.85	17.62
Rb	0.45	0.44	0.46	0.45	0.71	0.34	0.31	0.42	0.71	0.32	0.59	0.13	0.22
Sr	92.0	99.2	98.2	84.6	90.6	97.9	78.0	88.6	76.1	85.6	88.6	82.4	79.8
Y	26.0	26.4	27.4	21.0	22.9	43.3	16.4	15.8	13.3	16.1	23.2	33.6	35.1
Zr	51.4	65.8	69.0	44.0	55.2	148.5	33.2	28.5	23.3	38.1	44.2	80.0	80.7
Cs	0.004	0.004	0.004	0.003	0.007	0.003	0.006	0.002	0.007	0.000	0.003	0.005	0.004
Ba	9.62	9.74	10.83	21.94	17.47	9.52	8.89	8.04	9.07	6.57	9.75	7.02	6.31
La	2.33	2.60	2.93	2.26	1.83	3.65	2.01	1.65	1.41	1.88	1.82	2.84	2.87
Ce	7.35	7.50	7.94	7.08	5.54	11.21	5.80	4.86	3.59	5.04	5.48	8.41	9.01
Pr	1.27	1.22	1.37	1.28	0.92	2.03	0.91	0.81	0.55	0.78	0.95	1.44	1.53
Nd	6.94	6.53	7.14	6.57	5.31	10.68	4.61	4.13	3.14	4.07	5.27	8.01	8.21
Sm	2.44	2.39	2.51	2.22	1.93	3.97	1.53	1.51	1.16	1.40	1.92	2.94	3.03
Eu	0.97	1.09	0.99	0.90	0.83	1.14	0.75	0.70	0.60	0.72	0.80	1.05	1.15
Gd	3.34	3.29	3.50	3.01	2.73	5.65	2.16	1.97	1.67	1.99	2.82	4.17	4.38
Tb	0.64	0.64	0.68	0.52	0.54	1.05	0.39	0.37	0.32	0.37	0.53	0.79	0.85
Dy	4.12	4.11	4.34	3.36	3.59	6.89	2.55	2.33	2.02	2.45	3.53	5.37	5.71
Ho	0.91	0.96	0.96	0.73	0.77	1.54	0.57	0.55	0.46	0.57	0.81	1.19	1.23
Er	2.61	2.72	2.69	2.14	2.31	4.44	1.65	1.60	1.36	1.60	2.33	3.48	3.63
Yb	2.50	2.57	2.67	1.99	2.26	4.27	1.56	1.47	1.30	1.54	2.22	3.33	3.41
Lu	0.39	0.39	0.40	0.29	0.33	0.63	0.24	0.23	0.20	0.23	0.33	0.51	0.53
Hf	1.39	1.75	1.80	1.17	1.46	3.69	0.83	0.75	0.63	0.95	1.20	2.01	2.05
Th	0.13	0.13	0.15	0.11	0.12	0.36	0.08	0.07	0.05	0.08	0.09	0.21	0.19
U	0.04	0.05	0.05	0.03	0.04	0.11	0.03	0.03	0.02	0.05	0.03	0.07	0.06

Table T2 (continued).

Core, section:	230R-2	231R-3	231R-3	234R-1	234R-1
Interval (cm):	104–109	59–63	123–127	1–2	7–9
Depth (mbsf):	1485.54	1491.15	1491.79	1502.50	1502.57
Lithology:	G2	G2	G2	LDS	LDS
Rock name	Gabbronorite	Disseminated oxide olivine-bearing gabbronorite	Disseminated oxide gabbronorite	Type 8 metabasalt	Type 8 metabasalt
Major element oxide (wt%):					
SiO_2	50.48	49.78	50.78	49.05	49.58
TiO_2	1.16	1.15	0.96	1.38	1.37
Al_2O_3	14.38	14.65	14.65	13.91	13.86
FeO^{total}	9.49	9.96	9.09	12.16	12.1
MnO	0.16	0.17	0.16	0.16	0.17
MgO	8.25	8.95	8.63	8.28	8.27
CaO	12.7	12.55	12.78	12.09	12.04
Na_2O	2.56	2.39	2.41	2.41	2.44
K_2O	0.05	0.06	0.05	0.02	0.02
P_2O_5	0.08	0.04	0.03	0.02	0.03
LOI	0.88	0.61	0.57	0.94	0.42
Total:	100.18	100.29	100.10	100.43	100.29
Mg#:	60.8	61.6	62.9	54.8	54.9
Trace element (ppm):					
Sc	46.21	45.51	48.85	47.13	45.93
V	283.6	340.0	331.3	394.1	387.8
Ga	15.48	15.17	15.71	16.11	16.51
Rb	0.28	0.24	0.21	0.10	1.83
Sr	92.4	96.0	97.2	88.3	92.5
Y	31.6	21.5	25.4	18.5	19.8
Zr	62.3	34.1	32.0	15.5	19.7
Cs	0.003	0.002	–	0.003	0.008
Ba	9.03	7.33	7.20	5.16	5.60
La	2.48	1.37	1.45	0.74	0.72
Ce	7.28	4.11	4.83	2.40	2.41
Pr	1.28	0.73	0.89	0.46	0.50
Nd	7.42	3.97	4.87	2.97	3.03
Sm	2.92	1.73	2.01	1.36	1.49
Eu	1.00	0.85	0.86	0.70	0.73
Gd	4.03	2.43	3.14	2.14	2.32
Tb	0.78	0.48	0.57	0.44	0.45
Dy	5.02	3.28	3.82	2.90	3.12
Ho	1.12	0.76	0.88	0.64	0.72
Er	3.23	2.23	2.57	1.92	2.04
Yb	3.04	2.09	2.47	1.77	1.94
Lu	0.46	0.31	0.36	0.28	0.30
Hf	1.65	0.95	0.89	0.56	0.68
Th	0.15	0.07	0.10	0.02	0.02
U	0.04	0.02	0.03	0.01	0.01

Table T3. Average values of mineral compositions. (See table notes.) (Continued on next eight pages.)

Core, section, interval (cm)	Depth (mbsf)	Rock name	Phase	Replicates	Mode of occurrence	AP	Major element oxide (wt%)															
							SiO_2	TiO_2	Al_2O_3	Cr_2O_3	FeO	MnO	MgO	CaO	Na_2O	K_2O	NiO	BaO	Total	An%	Mg#	Fo
312-1256D-																						
172R-1, 12–14	1255.20	Type 3 metabasalt	Pl	*N* = 3	Phenocryst	Core	48.3	—	31.7	—	0.6	—	0.3	16.2	2.48	—	—	—	99.6	78.4		
				SD			1.2		0.9		0.1	—	0.0	1.0	0.59	—	—	—	0.2	5.1		
			Pl	*N* = 1	Phenocryst	Rim	51.0	—	29.6	—	0.7	—	0.3	14.1	3.62	—	—	—	99.4	68.2		
				SD																		
			Pl	*N* = 3	Lath	Core	50.6	—	30.7	—	0.7	—	0.3	14.9	3.13	—	—	—	100.4	72.5		
				SD			1.4		1.0		0.1		0.0	1.1	0.65				0.2	5.7		
			Pl	*N* = 3	Lath	Rim	50.7	—	30.6	—	0.6	—	0.3	14.8	3.23	—	—	—	100.3	71.8		
				SD			1.5		0.8		0.1		0.0	1.1	0.71				0.4	6.0		
			Cpx	*N* = 4	Phenocryst	Core	52.5	0.20	2.5	0.75	5.5	0.15	19.0	19.4	0.21	—	—	—	100.3		86.0	
				SD			0.2	0.04	0.5	0.14	0.1	0.01	0.5	0.4	0.01				0.1		0.2	
			Cpx	*N* = 4	Phenocryst	Rim	52.2	0.37	2.9	0.32	6.6	0.18	18.4	19.1	0.20	—	—	—	100.3		83.2	
				SD			0.4	0.09	0.6	0.03	0.7	0.04	0.3	0.9	0.01				0.4		1.7	
			Cpx	*N* = 6	Microlite	Core	51.9	0.40	3.3	0.29	6.9	0.20	18.4	18.7	0.22	—	—	—	100.4		82.5	
				SD			0.5	0.12	0.7	0.18	0.8	0.03	0.9	0.8	0.02				0.1		2.2	
174R-1, 32–34	1265.71	Type 3 metabasalt	Cpx	*N* = 3	Phenocryst	Core	51.5	0.29	3.5	1.02	5.4	0.12	18.3	19.5	0.19	—	—	—	99.9		85.7	
				SD			0.4	0.03	0.8	0.06	0.2	0.03	0.2	0.8	0.01				0.6		0.4	
			Cpx	*N* = 3	Phenocryst	Rim	51.9	0.44	2.8	0.34	7.1	0.12	18.1	18.5	0.18	—	—	—	99.5		82.0	
				SD			0.1	0.03	0.1	0.10	0.1		0.2	0.6	0.02				0.6		0.2	
			Cpx	*N* = 2	Microlite	Core	51.2	0.48	3.5	0.22	7.5	0.16	17.8	18.7	0.19	—	—	—	99.9		80.8	
				SD			0.2	0.02	0.3	0.08	0.9		0.1	1.1	0.00				0.6		1.7	
176R-1, 21–24	1276.29	Type 3 metabasalt	Pl	*N* = 1	Lath	Core	51.8	—	29.3	—	0.8	—	0.2	12.8	4.18	—	—	—	99.1	62.8		
				SD																		
			Pl	*N* = 1	Lath	Rim	49.2	—	31.0	—	0.6	—	0.3	15.3	2.84	—	—	—	99.3	74.9		
				SD																		
			Cpx	*N* = 6	Microlite	Core	51.0	0.58	3.8	0.18	8.5	0.20	16.4	18.9	0.38	—	—	—	100.1		77.3	
				SD			0.3	0.06	1.6	0.09	1.4	0.04	1.6	1.1	0.37				0.6		4.8	
178R-1, 0–3	1285.70	Type 3 metabasalt	Pl	*N* = 3	Lath	Core	50.9	—	30.0	—	0.6	—	0.3	14.4	3.43	—	—	—	99.7	69.8		
				SD			0.3		0.2		0.0		0.0	0.1	0.11				0.1	0.9		
			Pl	*N* = 2	Lath	Rim	52.4	—	29.0	—	0.7	—	0.2	13.0	4.20	—	—	—	99.6	63.1		
				SD			1.0		0.7		0.2		0.1	0.8	0.60				0.1	4.9		
			Cpx	*N* = 2	Microlite	Core	51.7	0.56	3.5	—	8.8	0.21	16.5	18.7	0.38	—	—	—	100.0		76.9	
				SD			0.0	0.05	0.2		0.2	0.00	0.2	0.0	0.00				0.1		0.6	
193R-1, 5–8	1353.10	Type 6 metabasalt	Pl	*N* = 3	Microlite	Core	53.2	—	28.2	—	0.9	—	0.1	11.7	4.89	—	—	—	99.1	57.0		
				SD			0.0		0.2		0.1		0.0	0.2	0.05				0.1	0.4		
			Cpx	*N* = 1	Phenocryst	Core	51.7	0.54	2.7	—	8.9	0.21	16.5	19.0	0.30	—	—	—	99.9		76.6	
				SD																		
194R-1, 29–33	1358.19	Type 7 metabasalt	Pl	*N* = 4	Lath	Core	51.9	0.07	29.4	—	0.8	—	0.1	13.3	4.03	—	—	—	99.7	64.6		
				SD			2.5		1.8		0.1		0.0	2.1	1.12				0.4	10.0		
			Pl	*N* = 2	Lath	Rim	51.9	—	29.5	—	0.7	—	0.1	13.3	4.10	—	—	—	99.8	64.3		
				SD			3.5		1.9		0.0		0.0	2.5	1.53				0.7	12.9		
			Cpx	*N* = 9	Microlite	Core	51.3	0.47	1.2	—	11.9	0.29	14.4	19.8	0.25	—	—	—	99.7		68.4	
				SD			0.3	0.04	0.1		0.3	0.04	0.1	0.6	0.01				0.4		0.5	

Table T3 (continued). (Continued on next page.)

Core, section, interval (cm)	Depth (mbsf)	Rock name	Phase	Replicates	Mode of occurrence	AP	Major element oxide (wt%)															
							SiO_2	TiO_2	Al_2O_3	Cr_2O_3	FeO	MnO	MgO	CaO	Na_2O	K_2O	NiO	BaO	Total	An%	Mg#	Fo
196R-1, 43–46	1364.13	Type 7 metabasalt	Pl	*N* = 4	Microlite	Core	54.6	—	27.5	—	0.8	—	0.0	11.0	5.35	0.08	—	—	99.5	53.3		
				SD			1.8		1.3		0.1		0.0	1.1	0.66				0.2	5.5		
			Pl	*N* = 4	Lath	Core	52.3	0.09	29.1	—	0.8	—	0.1	12.4	4.43	0.07	0.17	—	99.3	60.8		
				SD			2.8		1.8		0.0		0.0	2.5	1.43				0.2	12.6		
			Cpx	*N* = 1	Secondary-type	Core	53.2	—	0.4	—	8.3	0.32	15.2	21.3	0.20	—	—	—	99.1		76.5	
				SD																		
203R-1, 6–10	1374.89	Type 7 metabasalt	Pl	*N* = 22	Microlite	Core	54.8	—	27.3	—	0.8	—	0.1	10.5	5.53	—	—	—	99.3	51.2		
				SD			1.4		0.4		0.1		0.0	0.4	0.19				0.5	1.9		
			Cpx	*N* = 3	Phenocryst	Core	52.5	0.33	1.4	0.23	7.1	0.24	16.0	21.8	0.29	—	—	—	99.9		80.0	
				SD			0.7	0.23	0.7		1.4	0.02	0.9	1.2	0.04				0.5		3.7	
			Cpx	*N* = 3	Phenocryst	Rim	52.3	0.38	1.1	—	8.0	0.24	15.7	21.9	0.30	—	—	—	100.0		77.8	
				SD			0.2	0.20	0.5		0.9	0.04	0.3	1.4	0.05				0.2		2.3	
			Cpx	*N* = 9	Microgranular	Core	51.1	0.61	1.5	—	8.7	0.26	15.3	21.0	0.32	—	—	—	98.9		75.8	
				SD			0.5	0.05	0.1		0.4	0.03	0.3	0.5	0.02				0.6		0.9	
204R-1, 0–4	1377.30	Type 7 metabasalt	Pl	*N* = 9	Subhedral	Core	53.3	0.07	28.8	—	0.8	—	0.0	12.1	4.71	—	—	—	99.9	58.7		
				SD			1.7		1.1		0.1		0.0	1.5	0.78				0.3	6.8		
			Pl	*N* = 5	Subhedral	Rim	53.6	—	28.7	—	0.9	—	0.1	12.2	4.75	—	—	—	100.2	58.6		
				SD			0.7		0.3		0.1		0.0	0.5	0.19				0.3	1.9		
			Cpx	*N* = 4	Phenocryst	Core	51.6	0.47	1.3	—	12.5	0.33	14.2	19.4	0.24	—	—	—	100.2		67.0	
				SD			0.6	0.03	0.1		0.4	0.02	0.1	0.6	0.02				0.9		0.5	
			Cpx	*N* = 4	Microgranular	Core	51.4	0.61	2.1	—	12.7	0.34	13.9	19.1	0.40	—	—	—	100.8		66.1	
				SD			0.4	0.14	1.7		0.7	0.06	0.9	0.4	0.31				0.1		0.3	
			Opx	*N* = 8	Microgranular		52.3	0.33	0.7	—	23.4	0.53	21.7	1.9	—	—	—	—	100.9		62.3	
				SD			0.5	0.03	0.0		0.9	0.03	0.6	0.2	0.01				0.6		1.5	
214R-1, 19–21	1411.10	Gabbro 1	Pl	*N* = 4	Subhedral	Core	51.9	—	29.7	—	0.7	—	0.1	13.3	4.15	—	—	—	99.8	63.9		
				SD			1.5		0.9		0.1		0.0	1.2	0.62				0.4	5.5		
			Pl	*N* = 2	Subhedral	Rim	52.3	—	29.5	—	0.7	—	0.1	12.8	4.39	—	—	—	99.7	61.9		
				SD			3.1		1.6		0.2		0.0	2.1	1.28				0.9	10.7		
			Cpx	*N* = 9	Igneous-type	Core	51.0	0.46	3.4	0.73	7.2	0.12	16.8	20.2	0.24	—	—	—	100.1		80.7	
				SD	Subophitic domain		1.0	0.03	0.8	0.26	0.7	0.03	0.7	0.6	0.05				0.6		2.1	
			Cpx	*N* = 3	Igneous-type	Core	52.1	0.66	1.8	0.26	10.7	0.21	15.3	20.0	0.25	—	—	—	101.2		71.8	
				SD	Coarse-grained domain		0.2	0.06	0.1		0.3	0.02	0.5	0.5	0.02				0.7		1.2	
			Opx	*N* = 14	Anhedral		52.9	0.40	0.9	—	21.4	0.40	23.0	2.5	—	—	—	—	101.4		64.8	
				SD			0.3	0.03	0.1		2.1	0.06	1.2	0.9					0.8		3.7	
214R-2, 24–57	1412.60	Gabbro 1	Pl	*N* = 3	Subhedral	Core	49.1	—	31.3	—	0.4	—	0.1	15.2	3.06	—	—	—	99.3	73.4		
				SD			1.4		0.8		0.1		0.0	1.1	0.64				0.2	5.6		
			Cpx	*N* = 6	Igneous-type	Core	51.7	0.62	2.5	0.24	7.2	0.12	17.5	19.8	0.28	—	—	—	100.2		81.3	
				SD	Subophitic domain		0.6	0.05	0.5	0.06	0.5	0.02	0.5	0.7	0.06				0.5		1.5	
			Cpx	*N* = 3	Igneous-type	Core	50.7	0.60	2.7	0.28	9.0	0.15	16.3	19.6	0.24	—	—	—	99.6		76.3	
				SD	Coarse-grained domain		0.8	0.03	0.7		0.8	0.03	0.0	0.5	0.01				0.8		1.6	
214R-2, 78–81	1413.13	Gabbro 1	Pl	*N* = 2	Subhedral	Core	49.1	0.08	31.4	—	0.5	—	0.0	15.1	2.91	—	—	—	99.1	74.2		
				SD			1.1		1.0		0.0		0.0	1.0	0.70				0.2	5.9		
			Pl	*N* = 1	Subhedral	Rim	55.1	0.11	27.4	—	0.5	—	—	10.2	5.87	—	—	—	99.3	48.9		
				SD																		

Table T3 (continued). (Continued on next page.)

Core, section, interval (cm)	Depth (mbsf)	Rock name	Phase	Replicates	Mode of occurrence	AP	Major element oxide (wt%)															
							SiO_2	TiO_2	Al_2O_3	Cr_2O_3	FeO	MnO	MgO	CaO	Na_2O	K_2O	NiO	BaO	Total	An%	Mg#	Fo
			Cpx	*N* = 6	Igneous-type	Core	51.6	0.61	2.8	0.38	6.6	0.13	17.4	20.2	0.27	—	—	—	100.2		82.4	
				SD	Subophitic domain		0.3	0.05	0.2	0.10	0.3	0.03	0.3	0.5	0.01				0.3		0.6	
			Cpx	*N* = 6	Igneous-type	Core	51.4	0.59	2.1	—	9.3	0.19	16.2	19.5	0.29	—	—	—	99.9		75.5	
				SD	Coarse-grained domain		0.4	0.05	0.3		1.1	0.06	0.6	0.4	0.01				0.3		2.9	
214R-3, 18–21	1413.99	Gabbro 1	Cpx	*N* = 6	Igneous-type	Core	51.5	0.62	2.1	—	7.4	0.12	17.5	20.0	0.24	—	—	—	99.7		80.9	
				SD	Subophitic domain		0.5	0.18	0.5	0.04	0.2		0.3	0.1	0.01				0.3		0.3	
			Cpx	*N* = 3	Igneous-type	Core	50.8	0.87	1.6	—	13.1	0.30	14.5	18.9	0.24	—	—	—	100.0		66.3	
				SD	Coarse-grained domain		0.4	0.13	0.2		0.8	0.07	0.5	0.6	0.02				0.8		1.9	
215R-1, 20–23	1415.92	Gabbro 1	Pl	*N* = 1	Subhedral	Core	48.7	—	31.6	—	0.3	—	0.1	15.5	2.70	—	—	0.17	99.1	76.0		
				SD																		
			Pl	*N* = 1	Subhedral	Rim	49.5	—	30.9	—	0.4	—	0.1	14.9	3.13	—	—	—	99.2	72.5		
				SD																		
			Cpx	*N* = 9	Igneous-type	Core	51.8	0.54	2.4	0.22	6.7	0.22	17.7	20.2	0.22	—	—	0.16	100.2		82.4	
				SD	Subophitic domain		0.5	0.06	0.5	0.09	0.6	0.03	0.4	0.6	0.03			0.04	0.4		1.3	
			Cpx	*N* = 3	Igneous-type		50.8	0.63	2.2		11.1	0.32	16.4	17.6	0.20	—	—	0.19	99.6		72.4	
				SD	Coarse-grained domain		0.3	0.13	0.3		2.0	0.05	0.9	0.8	0.02			0.04	1.2		4.5	
			Opx	*N* = 8	Anhedral		51.8	0.43	0.6	—	23.7	0.52	21.4	2.1	—	—	—	0.17	100.9		61.6	
				SD			0.3	0.05	0.3		1.9	0.11	1.7	0.4				0.05	0.5		3.8	
			Ol	*N* = 3	Anhedral	Core	38.7	—	—	—	20.4	0.28	42.5	0.0	—	—	0.12	—	102.1			78.8
				SD			0.1				1.1	0.01	1.0	0.0			0.02		0.4			1.3
			Ol	*N* = 2	Anhedral	Rim	38.0	—	—	—	21.8	0.28	41.3	0.1	—	—	0.14	—	101.6			77.2
				SD			0.6				0.6	0.02	0.6	0.0			0.00		0.7			0.8
215R-2, 56–59	1417.69	Gabbro 1	Pl	*N* = 3	Subhedral	Core	50.6	0.07	30.8	—	0.6	—	0.1	14.1	3.45	—	—	—	99.8	69.3		
				SD			1.9		1.5		0.0		0.0	1.6	0.73				0.5	7.0		
			Pl	*N* = 3	Subhedral	Rim	55.2	—	27.3	—	0.6	—	0.0	10.2	5.71	0.13	—	—	99.2	49.7		
				SD			3.1		2.1		0.1		0.0	2.4	1.34				0.1	11.6		
			Cpx	*N* = 7	Igneous-type	Core	52.5	0.44	2.3	0.46	5.8	0.15	18.1	20.0	0.22	—	—	—	100.0		84.7	
				SD			0.5	0.04	0.5	0.24	0.7	0.03	0.4	0.4	0.02				0.5		1.6	
			Opx	*N* = 10	Anhedral		52.8	0.38	0.8	—	23.2	0.46	22.2	2.2	—	—	—	—	102.1		62.3	
				SD			0.6	0.10	0.1		2.6	0.10	1.1	1.6					0.7		2.9	
			Opx	*N* = 6	Within olivine pseudomorph		54.8	0.07	0.9	—	19.2	0.52	26.7	0.3	—	—	—	—	102.5		71.2	
				SD			0.5		0.5	—	0.6	0.08	0.5	0.1					0.5		0.9	
216R-1, 72–75	1418.62	Gabbro 1	Cpx	*N* = 9	Igneous-type	Core	52.2	0.42	1.8	0.19	6.3	0.20	18.0	20.4	0.20	—	—	0.16	99.9		83.7	
				SD			0.3	0.05	0.2	0.23	0.4	0.03	0.2	0.2	0.02			0.02	0.4		0.9	
			Opx	*N* = 8	Anhedral		52.4	0.41	1.1	—	19.7	0.42	23.4	2.6	—	—	—	0.21	100.3		67.9	
				SD			0.7	0.08	0.4		1.3	0.04	0.6	0.6				0.02	0.4		1.9	
216R-1, 138–142	1419.19	Gabbro 1	Pl	*N* = 8	Subhedral	Core	49.8	—	31.2	—	0.5	—	0.0	15.2	2.98	—	—	—	99.8	73.9		
				SD			1.1		0.9		0.1		0.0	1.0	0.53				0.5	4.6		
			Pl	*N* = 9	Subhedral	Rim	51.2	—	30.2	—	0.5	—	0.0	14.0	3.64	0.11	—	—	99.7	68.1		
				SD			1.9		1.3		0.0		0.0	1.5	0.85				0.3	7.4		
			Cpx	*N* = 10	Igneous-type	Core	52.9	0.46	2.0	0.35	5.8	—	17.9	20.8	0.20	—	—	—	100.6		84.5	
				SD			0.5	0.05	0.4	0.12	0.2		0.3	0.3	0.02				0.4		0.5	

Table T3 (continued). (Continued on next page.)

Core, section, interval (cm)	Depth (mbsf)	Rock name	Phase	Replicates	Mode of occurrence	AP	Major element oxide (wt%)															
							SiO_2	TiO_2	Al_2O_3	Cr_2O_3	FeO	MnO	MgO	CaO	Na_2O	K_2O	NiO	BaO	Total	An%	Mg#	Fo
217R-1, 94–97	1422.54	Gabbro 1	Pl	*N* = 7	Subhedral	Core	53.0	—	28.8	—	0.5	—	0.0	12.5	4.51	0.14	—	—	99.5	60.6		
				SD			2.3		1.4		0.1		0.0	1.7	1.03				0.4	8.7		
			Pl	*N* = 3	Subhedral	Rim	54.2	—	28.2	—	0.5	—	—	11.7	5.14	—	—	—	99.8	55.9		
				SD			2.4		1.4		0.0			1.9	1.14				0.4	9.6		
			Cpx	*N* = 8	Igneous-type	Core	52.5	0.48	2.3	0.49	5.5	—	17.7	20.9	0.21	—	—	—	100.1		85.2	
				SD			0.4	0.06	0.6	0.14	0.5		0.5	0.3	0.02				0.5		1.6	
218R-1, 1–3	1430	Gabbro 1	Cpx	*N* = 9	Igneous-type	Core	52.4	0.54	2.0	0.15	7.4	—	17.5	20.2	0.21	—	—	—	100.5		80.8	
				SD			0.5	0.17	0.2	0.11	1.9	0.01	0.6	1.2	0.02				0.4		2.1	
219R-1, 5–8	1430.05	Gabbro 1	Pl	*N* = 7	Subhedral	Core	50.2	—	30.7	—	0.5	—	0.0	14.6	3.39	—	—	—	99.5	70.4		
				SD			0.9		0.8		0.1		0.0	0.7	0.42				0.4	3.6		
			Pl	*N* = 6	Subhedral	Rim	53.2	0.09	28.7	—	0.6	—	0.1	12.0	4.79	—	—	—	99.4	58.1		
				SD			1.4		1.1		0.1		0.0	1.0	0.62				0.3	5.3		
			Cpx	*N* = 6	Igneous-type	Core	52.5	0.41	2.3	0.58	5.8	—	17.8	20.9	0.24	—	—	—	100.6		84.6	
				SD			0.3	0.08	0.5	0.28	0.5		0.3	0.2	0.03				0.3		1.2	
			Opx	*N* = 5	Anhedral		53.3	0.45	0.8	—	19.6	0.35	24.5	1.9	—	—	—	—	101.0		69.1	
				SD			0.4	0.05	0.1		1.0	0.06	0.6	0.1					0.8		1.6	
			Ol	*N* = 5	Anhedral	Core	36.9	—	—	—	30.3	0.40	34.7	0.1	—	—	0.08	—	102.4			67.1
				SD			0.4				0.7	0.01	0.7	0.0			0.01		0.4			0.9
			Ol	*N* = 5	Anhedral	Rim	37.0	—	—	—	31.2	0.42	33.9	0.0	—	—	0.08	—	102.6			66.0
				SD			0.4				0.8	0.02	0.4	0.0			0.01		0.8			0.8
222R-1, 73–78	1445.33	Gabbro 1	Pl	*N* = 7	Subhedral	Core	50.1	—	30.8	—	0.6	—	0.1	14.7	3.34	—	—	—	99.5	70.9		
				SD			1.4		1.0		0.1		0.0	1.2	0.66				0.2	5.7		
			Pl	*N* = 5	Subhedral	Rim	52.0	0.09	29.6	—	0.6	—	0.0	13.2	4.22	—	—	—	99.7	63.3		
				SD			1.2	0.01	0.8		0.1		0.0	1.1	0.62				0.5	5.4		
			Cpx	*N* = 6	Igneous-type	Core	52.3	0.46	2.6	0.60	5.3	—	17.7	20.8	0.25	—	—	—	100.1		85.6	
				SD			0.2	0.07	0.3	0.14	0.1		0.1	0.1	0.02				0.3		0.4	
			Opx	*N* = 7	Anhedral		53.5	0.62	1.2	—	16.5	0.29	26.3	2.1	—	—	—	—	100.6		74.0	
				SD			0.2	0.11	0.1		0.5	0.04	0.2	0.2	0.01				0.5		0.6	
			Ol	*N* = 3	Subhedral	Core	37.8	—	—	—	27.8	0.38	36.6	0.0	—	—	0.10	—	102.8			70.1
				SD			0.9				0.1	0.01	0.0	0.0			0.00		1.0			0.1
			Ol	*N* = 3	Subhedral	Rim	37.6	—	0.1	—	28.1	0.35	36.4	0.0	—	—	0.10	—	102.7			69.8
				SD			1.0		0.1		0.3	0.01	0.3	0.0			0.01		1.3			0.4
222R-2, 60–63	1446.70	Gabbro 1	Pl	*N* = 4	Subhedral	Core	50.0	—	31.6	—	0.5	—	0.0	15.0	3.08	—	—	—	100.2	72.9		
				SD			1.3		0.9		0.1		0.0	1.3	0.61				0.3	5.6		
			Pl	*N* = 5	Subhedral	Rim	51.8	0.10	30.4	—	0.5	—	0.0	13.5	3.92	—	—	—	100.2	65.6		
				SD			1.5	0.02	1.1		0.1		0.0	1.2	0.77				0.4	6.4		
			Cpx	*N* = 4	Igneous-type	Core	52.3	0.42	2.7	0.85	5.7	—	17.3	21.4	0.29	—	—	—	101.0		84.4	
				SD			0.3	0.03	0.3	0.14	0.5		0.2	0.0	0.04				0.2		1.3	
			Opx	*N* = 4	Anhedral		53.8	0.45	0.9	—	17.9	0.37	25.8	1.9	—	—	—	—	101.2		72.0	
				SD			0.1	0.03	0.1		0.4	0.06	0.2	0.1					0.5		0.3	
			Ol	*N* = 5	Subhedral	Core	37.3	—	—	—	30.3	0.37	34.6	0.0	—	—	0.08	—	102.7			67.1
				SD			0.6				0.2	0.01	0.1	0.0			0.01		0.8			0.2
			Ol	*N* = 5	Subhedral	Rim	36.8	—	—	—	30.4	0.38	34.5	0.0	—	—	0.08	—	102.3			67.0
				SD			0.7				0.4	0.00	0.4	0.0			0.00		0.9			0.4
223R-1, 8–12	1449.37	Gabbro 1	Pl	*N* = 5	Subhedral	Core	51.0	—	30.2	—	0.5	—	0.0	13.8	3.79	—	—	—	99.5	66.9		
				SD			1.3		1.0		0.1		0.0	1.1	0.71				0.3	6.0		
			Pl	*N* = 5	Subhedral	Rim	51.6	—	30.0	—	0.6	—	0.0	13.4	4.07	—	—	—	99.7	64.5		
				SD			0.9		0.8		0.1		0.0	0.9	0.49				0.3	4.3		

Table T3 (continued). (Continued on next page.)

Core, section, interval (cm)	Depth (mbsf)	Rock name	Phase	Replicates	Mode of occurrence	AP	Major element oxide (wt%)															
							SiO_2	TiO_2	Al_2O_3	Cr_2O_3	FeO	MnO	MgO	CaO	Na_2O	K_2O	NiO	BaO	Total	An%	Mg#	Fo
			Cpx	*N* = 5	Igneous-type	Core	52.6	0.39	2.1	0.33	6.1	0.11	17.8	21.0	0.20	—	—	—	100.7		83.9	
				SD			0.2	0.04	0.1	0.08	0.2	0.01	0.3	0.2	0.02				0.3		0.6	
			Opx	*N* = 8	Anhedral		53.3	0.54	1.1	—	17.3	0.32	25.9	1.9	—	—	—	—	100.6		72.7	
				SD			0.3	0.07	0.2		0.4	0.02	0.3	0.1					0.5		0.4	
			Ol	*N* = 5	Subhedral	Core	38.4	—	—	—	29.2	0.38	34.7	0.2	—	—	0.08	—	103.0			67.9
				SD			0.3				0.5	0.01	0.2	0.3			0.00		0.3			0.5
			Ol	*N* = 5	Subhedral	Rim	38.3	—	—	—	29.9	0.37	34.2	0.1	—	—	0.08	—	103.0			67.1
				SD			0.3				0.5	0.02	0.6	0.0			0.02		0.3			0.8
223R-2, 133–137	1452.11	Gabbro 1	Pl	*N* = 4	Subhedral	Core	52.2	—	29.5	—	0.5	—	0.0	12.9	4.34	—	—	—	99.6	62.1		
				SD			0.4		0.5		0.1		0.0	0.3	0.25				0.3	1.9		
			Pl	*N* = 5	Subhedral	Rim	52.8	—	29.1	—	0.7	—	0.0	12.3	4.68	—	—	—	99.6	59.1		
				SD			0.3		0.2		0.0		0.0	0.2	0.06				0.5	0.7		
			Pl	*N* = 7	Microgranular	Core	50.1	—	31.2	—	0.3	—	0.0	14.6	3.29	—	—	—	99.5	71.0		
				SD			1.7		1.0		0.1		0.0	1.4	0.76				0.3	6.7		
			Cpx	*N* = 3	Igneous-type	Core	51.6	0.62	1.9	—	8.3	0.18	15.2	21.8	0.34	—	—	—	100.3		76.5	
				SD			0.2	0.11	0.1		0.2	0.01	0.1	0.1	0.02				0.3		0.3	
			Cpx	*N* = 6	Secondary-type	Core	53.4	—	0.4	—	6.9	0.20	15.3	24.2	0.09	—	—	—	100.6		79.8	
				SD			0.3		0.2		0.7	0.04	0.4	0.8	0.04				0.5		2.0	
			Cpx	*N* = 7	Microgranular	Core	51.7	0.68	2.1	0.30	9.1	0.23	16.0	19.6	0.32	—	—	—	100.0		75.8	
				SD			0.3	0.13	0.1	0.10	0.4	0.04	0.4	0.8	0.03				0.6		0.8	
			Opx	*N* = 8	Anhedral		53.3	0.54	1.2	—	16.9	0.32	26.0	2.2	—	—	—	—	100.6		73.2	
				SD			0.3	0.05	0.1		0.6	0.04	0.3	0.3					0.6		0.8	
			Ol	*N* = 8	Interstitial	Core	38.0	0.05	—	—	29.1	0.37	34.4	0.1			0.07		102.0			67.8
				SD			0.2	0.01	—	—	0.2	0.03	0.2	0.0			0.01		0.3			0.3
			Ol	*N* = 5	Interstitial	Rim	38.0	0.06	—	—	29.1	0.37	34.3	0.1			0.07		101.9			67.7
				SD			0.2	0.00	—	—	0.4	0.03	0.4	0.0			0.01		0.4			0.5
226R-1, 0–4	1463.90	Type 8 metabasalt; UDS	Pl	*N* = 2	Subhedral	Core	52.5	—	29.6	—	0.4	—	—	12.5	4.37	—	—	—	99.5	61.4		
				SD			0.3		0.0		0.1			0.4	0.06				0.0	0.4		
			Pl	*N* = 3	Subhedral	Rim	54.5	—	28.3	—	0.4	—	—	11.2	5.38	—	—	—	100.0	53.5		
				SD			1.4		0.7		0.0			0.9	0.54				0.3	4.5		
			Cpx	*N* = 7	Secondary-type	Core	52.5	0.16	0.6	—	10.0	0.23	14.4	22.1	0.24	—	—	—	100.4		71.9	
				SD			0.3	0.11	0.2		0.4	0.04	0.3	0.7	0.06				0.3		0.8	
230R-1, 19–21	1483.19	Gabbro 2	Pl	*N* = 7	Subhedral	Core	54.3	—	28.3	—	0.6	—	0.1	11.0	5.27	—	—	—	99.6	53.6		
				SD			0.5		0.3		0.1		0.0	0.5	0.24				0.4	2.2		
			Pl	*N* = 5	Subhedral	Rim	55.7	—	27.3	—	0.6	—	0.0	10.0	6.00	—	—	—	99.7	47.9		
				SD			1.7		0.9		0.1		0.0	1.0	0.68				0.5	5.4		
			Cpx	*N* = 7	Amphibole-type	Core	52.5	0.16	0.6	—	10.0	0.23	14.4	22.1	0.24	—	—	—	100.4		71.9	
				SD			0.3	0.07	0.2		0.4	0.04	0.3	0.7	0.06				0.3		0.8	
			Opx	*N* = 9	granular		52.6	0.35	0.8	—	22.5	0.46	22.2	1.9	—	—	—	—	100.9		63.7	
				SD			0.2	0.08	0.2		0.6	0.04	0.3	0.3					0.4		0.8	
230R-1, 81–84	1483.81	Gabbro 2	Pl	*N* = 5	Subhedral	Core	54.3	0.09	28.2	—	0.5	—	0.1	11.1	5.40	—	—	—	99.7	53.3		
				SD			0.5	0.01	0.2		0.2		0.1	0.2	0.20				0.4	1.4		
			Pl	*N* = 5	Subhedral	Rim	56.7	—	26.7	—	0.4	—	—	9.2	6.35	—	—	—	99.4	44.3		
				SD			1.5		1.4		0.1			1.7	0.87				0.8	8.0		
			Cpx	*N* = 3	Igneous-type	Core	51.7	0.57	1.3	—	10.6	0.26	14.9	20.6	0.34	—	—	—	100.5		71.6	
				SD			0.4	0.09	0.3		0.4	0.03	0.1	0.4	0.04				0.6		0.9	
			Cpx	*N* = 6	Secondary-type	Core	53.2	0.07	0.3	—	8.4	0.15	14.3	22.9	0.64	—	—	—	100.2		75.2	

Table T3 (continued). (Continued on next page.)

Core, section, interval (cm)	Depth (mbsf)	Rock name	Phase	Replicates	Mode of occurrence	AP	Major element oxide (wt%)														
							SiO_2	TiO_2	Al_2O_3	Cr_2O_3	FeO	MnO	MgO	CaO	Na_2O	K_2O	NiO	BaO	Total	An%	Mg#	Fo
				SD			0.3	0.01	0.1		0.9	0.05	0.4	0.3	0.13				0.4		2.4	
			Opx	*N* = 16	granular		52.5	0.39	0.8	—	22.1	0.45	22.4	1.9	—	—	—	—	100.9		64.4	
				SD			0.2	0.03	0.1		0.7	0.05	0.5	0.1					0.6		1.1	
230R-1, 139–142	1484.38	Gabbro 2	Pl	*N* = 5	Subhedral	Core	53.2	0.09	28.7	—	0.7	0.11	0.1	12.0	4.79	—	—	—	99.7	58.0		
				SD			0.8	0.00	0.7		0.1	0.00	0.0	0.7	0.44				0.3	3.7		
			Pl	*N* = 3	Subhedral	Rim	53.8	0.08	28.2	—	0.7	—	0.1	11.5	5.10	—	—	—	99.6	55.4		
				SD			0.8	0.01	0.8		0.1		0.0	0.9	0.44				0.3	4.0		
			Cpx	*N* = 6	Igneous-type	Core	52.8	0.07	0.4	—	10.1	0.27	14.0	22.7	0.24	—	—	—	100.7		71.2	
				SD			0.3	0.04	0.2		0.6	0.02	0.2	0.4	0.06				0.4		1.5	
			Cpx	*N* = 6	Amphibole-type	Core	51.9	0.52	1.2	—	10.2	0.25	14.7	20.9	0.41	—	—	—	100.3		72.1	
				SD			0.7	0.21	0.5		1.0	0.04	0.4	0.9	0.17				0.6		1.7	
230R-2, 32–36	1484.58	Gabbro 2	Pl	*N* = 5	Subhedral	Core	51.2	—	30.2	—	0.6	—	0.1	13.6	3.91	—	—	—	99.7	65.8		
				SD			0.4		0.4		0.1		0.0	0.5	0.19				0.4	1.9		
			Pl	***N*** = 3	Subhedral	Rim	53.1	—	29.0	—	0.5	—	0.0	11.9	4.79	0.08	—	—	99.5	57.9		
				SD			0.2		0.1		0.1		0.0	0.2	0.15				0.1	1.2		
			Cpx	*N* = 6	Igneous-type	Core	52.1	0.30	0.9	—	10.3	0.34	14.6	21.6	0.30	—	—	—	100.6		71.7	
				SD			0.3	0.03	0.3		0.5	0.05	0.3	0.3	0.05				0.3		1.3	
			Cpx	*N* = 6	Amphibole-type	Core	52.8	0.07	0.4	—	10.1	0.27	14.0	22.7	0.24	—	—	—	100.7		71.2	
				SD			0.3	0.04	0.2		0.6	0.02	0.2	0.4	0.06				0.4		1.5	
			Opx	*N* = 13	Anhedral		52.7	0.50	0.8	—	21.8	0.54	22.9	2.0	—	—	—	—	101.3		65.2	
				SD			0.4	0.07	0.2		0.9	0.04	0.5	0.2					0.5		1.4	
230R-2, 104–109	1485.54	Gabbro 2	Pl	*N* = 5	Subhedral	Core	52.1	—	29.4	—	0.6	—	0.1	12.8	4.30	—	—	—	99.4	62.3		
				SD			0.8		0.8		0.1		0.0	0.7	0.49				0.4	3.9		
			Pl	*N* = 3	Subhedral	Rim	53.1	—	28.8	—	0.6	—	0.0	12.1	4.72	—	—	—	99.5	58.6		
				SD			1.4		1.0		0.1		0.0	1.4	0.77				0.3	6.8		
			Cpx	*N* = 14	Igneous-type	Core	52.1	0.40	1.1	—	10.2	0.22	14.7	21.5	0.27	—	—	—	100.7		72.0	
				SD			0.6	0.23	0.5		1.4	0.06	0.6	1.5	0.03				0.6		2.8	
			Cpx	*N* = 2	Amphibole-type	Core	52.4	0.20	1.0	—	10.0	0.22	14.3	21.7	0.28	—	—	—	100.3		72.0	
				SD			0.5	0.00	0.5		1.3	0.01	0.0	1.2	0.02				0.0		2.6	
			Opx	*N* = 8	Anhedral		53.0	0.49	0.9	—	21.1	0.39	23.8	2.0	—	—	—	—	101.8		66.9	
				SD			0.3	0.05	0.1		1.1	0.03	0.6	0.1					0.5		1.7	
231R-1, 19–22	1487.90	Gabbro 2	Pl	*N* = 7	Subhedral	Core	50.4	0.09	30.7	—	0.6	—	0.0	14.1	3.54	0.08	0.22	—	99.5	68.7		
				SD			0.3	0.02	0.2		0.1		0.0	0.5	0.22				0.4	2.1		
			Pl	*N* = 5	Subhedral	Rim	52.7	0.07	29.2	—	0.5	—	0.0	12.1	4.69	0.08	—	—	99.5	58.8		
				SD			1.5	0.00	0.9		0.1		0.0	1.4	0.68	0.00			0.2	6.2		
			Cpx	*N* = 7	Igneous-type	Core	51.9	0.57	1.7	—	10.2	0.21	15.7	20.3	0.21	—	—	—	101.0		73.4	
				SD			0.5	0.08	0.4		2.1	0.08	1.4	0.6	0.03				0.3		5.6	
			Cpx	*N* = 4	Amphibole-type	Core	52.5	0.24	1.1	—	9.3	0.24	14.8	21.7	0.30	—	—	—	100.3		73.9	
				SD			0.5	0.11	0.6		0.2	0.03	0.2	1.0	0.06				0.8		0.3	
			Opx	*N* = 7	Anhedral		52.9	0.56	0.9	—	20.5	0.39	24.2	2.0	—	—	—	—	101.8		67.8	
				SD			0.2	0.03	0.0		0.6	0.05	0.3	0.0					0.8		0.6	
231R-2, 35–39	1489.54	Gabbro 2	Pl	*N* = 5	Subhedral	Core	50.6	0.08	30.4	—	0.5	—	0.0	13.8	3.68	—	—	—	99.2	67.5		
				SD			1.4		0.9		0.1		0.0	1.2	0.70				0.3	6.1		
			Pl	*N* = 5	Subhedral	Rim	52.9	—	28.8	—	0.5	—	0.1	11.9	4.87	—	—	—	99.1	57.4		
				SD			0.6		0.4		0.1		0.1	0.6	0.27				0.1	2.5		
			Cpx	*N* = 15	Igneous-type	Core	51.2	0.68	1.7	0.15	10.3	0.23	15.1	20.0	0.27	—	—	—	99.8		72.4	
				SD			0.4	0.14	0.3	0.05	1.2	0.07	0.7	0.8	0.04				0.7		3.0	
			Cpx	*N* = 6	Amphibole-type	Core	51.7	0.36	1.9	0.32	9.0	0.20	14.8	21.4	0.26	—	—	—	100.0		74.5	

Table T3 (continued). (Continued on next page.)

Core, section, interval (cm)	Depth (mbsf)	Rock name	Phase	Replicates	Mode of occurrence	AP	Major element oxide (wt%)															
							SiO_2	TiO_2	Al_2O_3	Cr_2O_3	FeO	MnO	MgO	CaO	Na_2O	K_2O	NiO	BaO	Total	An%	Mg#	Fo
				SD			0.5	0.20	0.8	0.11	1.6	0.06	1.0	1.3	0.03				0.3		4.4	
			Opx	*N* = 9	Anhedral		52.6	0.50	0.9	—	20.0	0.39	23.6	2.1	—	—	—	—	100.3		67.7	
				SD			0.3	0.05	0.1		0.7	0.05	0.3	0.1					0.4		1.0	
231R-2, 95–98	1490.14	Gabbro 2	Pl	*N* = 3	Subhedral	Core	50.2	0.08	30.9	—	0.6	—	0.1	14.3	3.40	—	—	—	99.6	69.9		
				SD			0.5		0.1		0.1		0.0	0.4	0.17				0.4	1.6		
			Pl	*N* = 2	Subhedral	Rim	53.2	0.09	28.6	—	0.7	—	0.1	11.4	4.94	—	—	—	99.1	56.1		
				SD			0.9	0.02	0.5		0.2		0.0	0.8	0.46				0.2	4.0		
			Cpx	*N* = 8	Igneous-type	Core	51.9	0.55	2.2	0.23	7.2	0.14	17.3	20.5	0.25	—	—	—	100.5		81.0	
				SD			0.4	0.12	0.2	0.18	1.2	0.03	0.9	0.5	0.04				0.3		3.4	
			Cpx	*N* = 5	Amphibole-type	Core	52.4	0.16	0.6	—	10.0	0.22	14.4	22.1	0.23	—	—	—	100.3		72.1	
				SD			0.3	0.04	0.2		0.9	0.02	0.5	0.6	0.08				0.3		2.4	
			Opx	*N* = 6	Anhedral		52.7	0.54	0.9	—	20.9	0.42	23.6	2.1	—	—	—	—	101.6		66.8	
				SD			0.3	0.03	0.1		0.2	0.03	0.3	0.2					0.4		0.4	
231R-3, 59–63	1491.15	Gabbro 2	Pl	*N* = 3	Subhedral	Core	50.9	0.10	29.9	—	0.6	—	0.1	13.5	3.94	—	—	—	99.1	65.4		
				SD			3.0	0.02	1.9		0.0		0.0	2.2	1.24				0.2	10.9		
			Pl	*N* = 1	Subhedral	Rim	53.3	0.08	28.5	—	0.4	—	0.0	11.7	5.07	—	—	—	99.2	56.1		
				SD																		
			Cpx	*N* = 6	Igneous-type	Core	52.2	0.43	2.0	0.27	7.3	0.14	17.3	20.4	0.24	—	—	—	100.5		80.8	
				SD			0.3	0.04	0.1	0.04	0.9	0.04	0.5	0.4	0.02				0.4		2.2	
			Cpx	*N* = 3	Amphibole-type	Core	52.7	0.16	0.8	—	8.7	0.20	14.9	22.8	0.22	—	—	—	100.6		75.5	
				SD			0.3	0.02	0.3		0.3	0.05	0.2	0.4	0.01				0.5		0.8	
			Opx	*N* = 6	Anhedral		52.9	0.53	0.8	—	20.8	0.38	23.8	2.1	—	—	—	—	101.5		67.1	
				SD			0.4	0.12	0.1		0.7	0.04	0.3	0.4					0.7		0.9	
			Ol	*N* = 2	Interstitial	Core	38.0	—	0.0	—	29.4	0.44	34.3	0.0			0.07		102.3			67.6
				SD			0.1	—	—	—	0.0	0.00	0.4	0.0			0.00		0.4			0.2
			Ol	*N* = 2	Interstitial	Rim	38.1	—	0.0	—	28.7	0.44	34.8	0.0			0.06		102.1			68.4
				SD			0.0	—	—	—	0.1	0.05	0.4	0.0			0.00		0.4			0.2
231R-4, 70–74	1492.63	Gabbro 2	Pl	*N* = 8	Subhedral	Core	51.7	0.12	29.8	—	0.5	—	0.0	13.0	4.14	—	—	—	99.3	63.5		
				SD			1.1		0.8		0.1		0.0	0.9	0.49				0.2	4.4		
			Pl	*N* = 1	Subhedral	Rim	52.7	—	28.8	—	0.8	—	0.0	12.1	4.66	—	—	—	99.2	59.0		
				SD																		
			Cpx	*N* = 7	Igneous-type	Core	51.5	0.64	1.9	0.23	8.7	0.18	15.5	21.0	0.24	—	—	—	100.0		75.9	
				SD			0.4	0.16	0.4	0.07	1.6	0.05	1.4	0.7	0.02				0.5		4.7	
			Cpx	*N* = 6	Amphibole-type	Core	52.8	0.09	0.5	—	7.9	0.14	15.1	22.8	0.31	—	—	—	99.8		77.3	
				SD			0.1	0.01	0.2		1.0	0.02	0.5	0.7	0.13				0.3		2.7	
			Opx	*N* = 9	Anhedral		52.6	0.48	1.0	—	19.9	0.36	23.9	1.9	—	—	—	—	100.4		68.1	
				SD			0.1	0.06	0.1		0.4	0.06	0.2	0.2					0.4		0.6	
			Ol	*N* = 3	Anhedral	Core	38.8	—	—	—	25.1	0.41	37.6	0.0			0.08		102.0			72.7
				SD			0.2	—	—	—	0.7	0.01	0.5	0.0			0.01		0.1			0.8
			Ol	*N* = 3	Anhedral	Rim	39.1	—	0.0	—	24.5	0.38	38.4	0.0			0.08		102.5			73.6
				SD			0.5	—	0.0	—	0.8	0.03	0.9	0.0			0.00		0.7			1.1
232R-1, 36–39	1493.26	Gabbro 2	Pl	*N* = 1	Subhedral	Core	54.2	—	27.7	—	0.6	—	0.1	11.0	5.17	—	—	—	98.9	54.0		
				SD																		
			Pl	*N* = 1	Subhedral	Rim	53.4	—	28.4	—	0.4	—	0.0	11.6	5.13	—	—	—	99.0	55.6		
				SD																		
			Cpx	*N* = 3	Igneous-type	Core	51.7	0.55	1.7	—	10.6	0.29	14.9	20.4	0.39	—	—	—	100.8		71.4	
				SD			0.6	0.16	0.4		0.9	0.03	0.4	0.7	0.17				0.4		1.2	
			Cpx	*N* = 6	Amphibole-type	Core	52.4	0.26	1.8	—	8.3	0.23	15.1	21.8	0.50	—	—	—	100.5		76.4	
				SD			0.3	0.07	1.1		0.5	0.03	0.6	1.0	0.29				0.6		1.5	

Table T3 (continued). (Continued on next page.)

Core, section, interval (cm)	Depth (mbsf)	Rock name	Phase	Replicates	Mode of occurrence	AP	Major element oxide (wt%)															
							SiO_2	TiO_2	Al_2O_3	Cr_2O_3	FeO	MnO	MgO	CaO	Na_2O	K_2O	NiO	BaO	Total	An%	Mg#	Fo
			Opx	*N* = 6	Anhedral		52.9	0.42	0.8	—	20.1	0.42	24.5	1.9	—	—	—	—	101.1		68.5	
				SD			0.5	0.17	0.2		0.5	0.03	0.5	0.4					0.6		1.0	
			Ol	*N* = 11	Anhedral	Core	38.4	—	0.0	—	27.5	0.40	36.0	0.0			0.06		102.4			70.0
				SD			0.2	—	0.0	—	0.4	0.01	0.4	0.0			0.01		0.3			0.6
			Ol	*N* = 7	Anhedral	Rim	38.5	—	0.0	—	27.1	0.40	36.4	0.1			0.07		102.6			70.6
				SD			0.2	—	0.0	—	0.4	0.01	0.4	0.0			0.01		0.2			0.5
232R-1, 78–82	1493.68	Gabbro 2	Pl	*N* = 6	Subhedral	Core	51.1	—	30.1	—	0.6	—	0.0	13.6	3.82	—	—	—	99.3	66.3		
				SD			0.7		0.6		0.0		0.0	0.7	0.52				0.1	4.2		
			Pl	*N* = 5	Subhedral	Rim	55.4	—	27.6	—	0.4	—	0.0	10.1	5.96	—	—	—	99.5	48.4		
				SD			1.1		0.8		0.1		0.0	1.0	0.50				0.3	4.5		
			Cpx	*N* = 5	Igneous-type	Core	51.4	0.62	1.8	0.18	9.3	0.24	15.6	20.6	0.30	—	—	—	100.1		74.9	
				SD			0.3	0.10	0.2		0.5	0.07	0.1	0.6	0.02				0.4		0.8	
			Cpx	*N* = 14	Amphibole-type	Core	52.5	0.10	0.6	—	8.5	0.23	14.7	23.0	0.21	—	—	—	100.1		75.5	
				SD			0.4	0.04	0.2		0.6	0.06	0.3	0.3	0.06				0.4		1.6	
			Opx	*N* = 14	Anhedral		52.8	0.46	0.9	—	18.9	0.40	24.8	2.0	—	—	—	—	100.3		70.1	
				SD			0.2	0.04	0.2		0.8	0.03	0.4	0.1					0.4		1.2	
			Opx	*N* = 3	Granular		54.2	0.27	0.8	—	17.1	0.38	27.3	0.9	—	—	—	—	101.0		72.6	
				SD			0.9	0.08	0.3		1.2	0.03	1.7	0.8					0.4		0.4	
232R-2, 10–14	1494.08	Gabbro 2	Pl	*N* = 1	Subhedral	Core	52.2	—	29.2	—	0.6	—	0.1	12.3	4.43	—	—	—	98.8	60.5		
				SD																		
			Pl	*N* = 1	Subhedral	Rim	54.4	—	28.1	—	0.5	—	0.1	10.6	5.42	—	—	—	99.1	51.9		
				SD																		
			Cpx	*N* = 7	Amphibole-type	Core	53.2	0.14	0.7	—	9.0	0.23	15.0	22.4	0.33	—	—	—	101.1		74.9	
				SD			0.4	0.10	0.4		0.6	0.05	0.6	0.9	0.09				0.3		1.7	
			Opx	*N* = 8	Anhedral		53.1	0.48	0.7	—	20.7	0.45	24.5	1.8	—	—	—	—	102.0		67.9	
				SD			0.2	0.02	0.1		0.9	0.05	0.5	0.2					0.4		1.4	
232R-2, 73–76	1494.71	Gabbro 2	Pl	*N* = 4	Subhedral	Core	49.4	—	31.0	—	0.7	—	0.1	15.1	3.04	—	—	—	99.4	73.3		
				SD			1.0		0.6		0.1		0.0	0.6	0.40				0.2	3.4		
			Pl	*N* = 3	Subhedral	Rim	50.8	—	30.1	—	0.7	—	0.1	13.7	3.70	—	—	—	99.1	67.2		
				SD			1.7		0.9		0.2		0.0	1.5	0.83				0.1	7.3		
			Cpx	*N* = 2	Igneous-type	Core	52.9	0.30	1.9	0.56	5.5	0.18	18.3	20.8	0.20	—	—	—	100.7		85.5	
				SD			0.0	0.01	0.0	0.07	0.0	0.01	0.0	0.0	0.00				0.1		0.0	
			Cpx	*N* = 3	Amphibole-type	Core	52.1	0.44	1.4	0.18	9.9	0.25	15.1	20.6	0.25	—	—	—	100.3		73.2	
				SD			0.7	0.17	0.6		1.4	0.06	0.5	1.3	0.01				0.6		3.3	
			Opx	*N* = 8	Anhedral		53.3	0.48	0.9	—	18.7	0.40	25.4	1.9	—	—	—	—	101.1		70.8	
				SD			0.3	0.06	0.2		0.9	0.06	0.8	0.2					0.6		1.6	
233R-1, 4–7	1497.50	Type 8 metabasalt; LDS	Pl	*N* = 3	Subhedral	Core	53.4	—	28.7	—	0.5	—	0.0	11.6	4.96	—	—	—	99.3	56.4		
				SD			1.3		0.8		0.0		0.0	0.9	0.45				0.4	4.0		
			Pl	*N* = 2	Subhedral	Rim	54.1	—	28.2	—	0.6	—	0.0	11.1	5.34	—	—	—	99.5	53.4		
				SD			0.5		0.0		0.0		0.0	0.0	0.06				0.6	0.1		
			Cpx	*N* = 2	Igneous-type	Core	51.3	0.62	1.7	—	10.4	0.25	15.1	20.4	0.35	—	—	—	100.2		72.1	
				SD			0.5	0.09	0.4		0.5	0.04	0.1	0.7	0.06				0.7		0.9	
			Cpx	*N* = 3	Amphibole-type	Core	53.5	0.11	0.5	—	7.2	0.18	15.7	22.9	0.32	—	—	—	100.6		79.7	
				SD			0.1	0.02	0.1		0.1	0.07	0.1	0.3	0.04				0.3		0.3	
			Cpx	*N* = 3	Secondary-type	Core	53.2	0.08	0.3	—	8.6	0.16	14.8	22.7	0.55	—	—	—	100.5		75.5	
				SD			0.1	0.02	0.1		1.0	0.03	0.7	0.5	0.22				0.4		2.9	
			Opx	*N* = 15	Microgranular		52.9	0.39	0.8	—	20.5	0.41	23.8	1.9	—	—	—	—	100.9		67.4	

Table T3 (continued).

Core, section, interval (cm)	Depth (mbsf)	Rock name	Phase	Replicates	Mode of occurrence	AP	Major element oxide (wt%)														
							SiO_2	TiO_2	Al_2O_3	Cr_2O_3	FeO	MnO	MgO	CaO	Na_2O	K_2O	NiO	BaO	Total	An%	Mg#	Fo
				SD			0.2	0.04	0.1		0.4	0.04	0.2	0.2					0.6		0.5	
234R-1, 1–2	1502.50	Type 8 metabasalt; LDS	Pl	*N* = 2	Phenocryst	Core	49.8	—	30.8	—	0.8	—	0.0	14.7	3.17	—	—	—	99.3	72.0		
				SD			0.3		0.1		0.1		0.0	0.1	0.14				0.1	0.8		
			Pl	*N* = 2	Phenocryst	Rim	54.5	0.09	28.1	—	0.7	—	0.0	11.2	5.24	—	—	—	99.8	54.1		
				SD			0.4	—	0.1		0.2		0.0	0.0	0.23				0.4	1.2		
			Pl	*N* = 5	Microgranular	Core	54.3	—	28.1	—	0.6	—	0.0	11.0	5.46	—	—	—	99.5	52.7		
				SD			0.3		0.2		0.0		0.0	0.2	0.08				0.3	0.7		
			Cpx	*N* = 4	Phenocryst	Core	51.4	0.54	1.6	0.33	9.9	0.22	14.9	21.1	0.30	—	—	—	100.2		72.8	
				SD			0.3	0.14	0.3	0.17	0.5	0.02	0.1	0.4	0.06				0.4		1.1	
			Cpx	*N* = 1	Phenocryst	Rim	51.4	0.63	1.8	—	9.6	0.24	14.6	21.5	0.32	—	—	—	100.3		73.1	
				SD																		
			Cpx	*N* = 6	Microgranular	Core	51.7	0.54	1.3	—	9.9	0.26	15.0	21.2	0.24	—	—	—	100.2		73.1	
				SD			0.3	0.12	0.2		0.6	0.05	0.2	0.7	0.03				0.4		0.9	
234R-1, 7–9	1502.57	Type 8 metabasalt; LDS	Pl	*N* = 3	Phenocryst	Core	50.7	—	30.4	—	0.6	—	—	14.0	3.47	—	—	—	99.3	69.1		
				SD			0.2		0.2		0.1			0.2	0.06				0.3	0.6		
			Pl	*N* = 2	Phenocryst	Rim	52.6	—	29.3	—	0.5	—	0.0	12.5	4.42	—	—	—	99.3	61.0		
				SD			2.9		1.6		0.0		0.0	2.2	1.31				0.4	11.2		
			Pl	*N* = 2	Microgranular	Core	54.3	—	28.1	—	0.6	—	0.0	11.2	5.17	—	—	—	99.4	54.6		
				SD			0.6		0.2		0.0		0.0	0.2	0.34				0.5	2.1		
			Cpx	*N* = 1	Phenocryst	Core	50.8	0.58	1.5	—	9.2	0.25	14.5	22.0	0.32	—	—	—	99.2		73.8	
				SD																		
			Cpx	*N* = 1	Phenocryst	Rim	51.4	0.54	1.3	—	9.6	0.23	14.9	21.3	0.30	—	—	—	99.6		73.4	
				SD																		
			Cpx	*N* = 6	Microgranular	Core	51.8	0.56	1.3	—	10.0	0.25	15.0	20.9	0.27	—	—	—	100.0		72.7	
				SD			0.3	0.13	0.1		0.5	0.05	0.2	0.5	0.03				0.5		0.9	
			Opx	*N* = 12	Microgranular		52.5	0.41	0.8	—	21.4	0.43	23.1	1.7	—	—	—	—	100.5		65.8	
				SD			0.3	0.04	0.1		0.4	0.04	0.3	0.2					0.6		0.6	
Detection limits:																						
Pl, Cpx, and Opx							0.0	0.07	0.0	0.14	0.1	0.10	0.0	0.0	0.06	0.07	0.12	0.16				
Ol							0.0	0.04	0.0	0.04	0.0	0.02	0.0	0.0			0.02					

Notes: Replicate *N* = number of analyses and SD = standard deviation of the mean of replicates. AP = analyzed position in the crystal. An% = anorthite mol%. Mg# = 100 × Mg/(Mg + Fe), Fo = forsterite mol%. UDS = upper dike screen, LDS = lower dike screen. Pl = plagioclase, Cpx = clinopyroxene, Opx = orthopyroxene, Ol = olivine. — = below detection limit, blank cell = not analyzed.